Temperature and Abundance measurements in galaxy clusters with high energy resolution spectroscopy

Marie Kondo
Saitama University

Galaxy Clusters

Hot (10^7-10^8K) X-ray emitting gas (ICM) fills the space between galaxies.

Abundances in the ICM enable us to understand the chemical evolution history and evolution process of the clusters.

- ✓ What kind of stars synthesized the heavy elements?

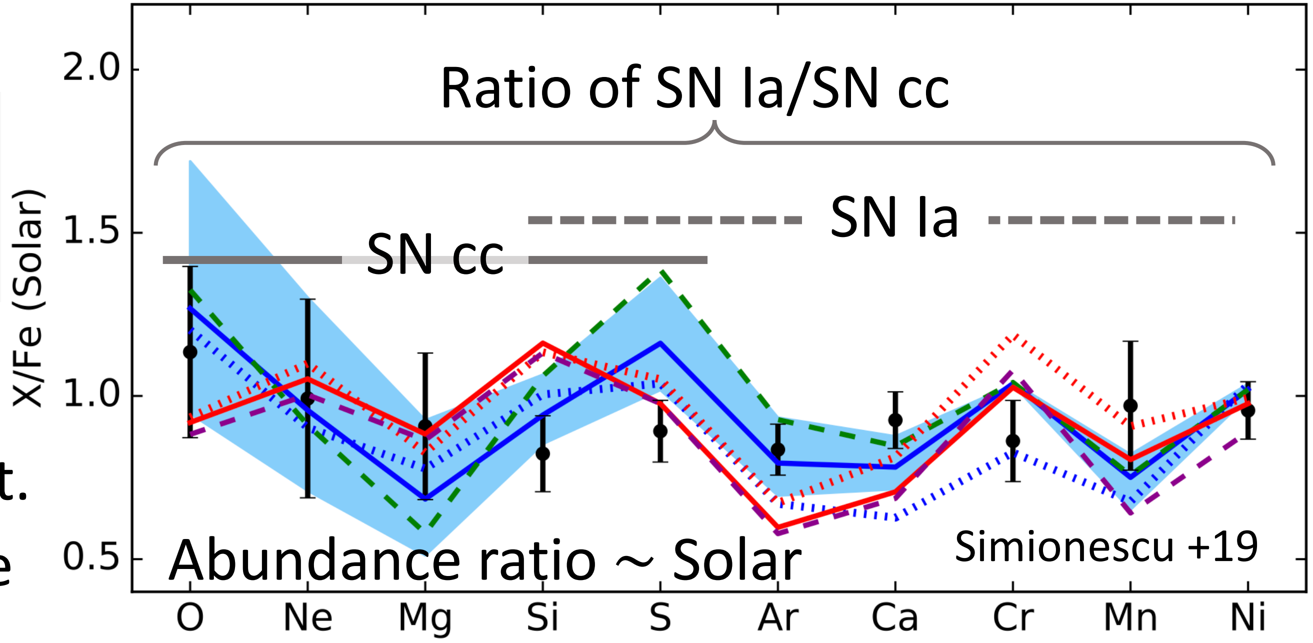

Measurement of temperature structure is directly linked to abundance measurement.

We need to measure abundances of all the metals from O to Fe, Ni.

Previous study

- ✓ Perseus cluster (Hitomi/SXS, XMM/RGS)
  Simionescu +19 (Not spatially resolved spectra)
- ✓ CHEmical Evolution RGS Sample(CHEERS)
  e.g., de Plaa +17, Mao+19, Fukushima+23

Combination of several detectors

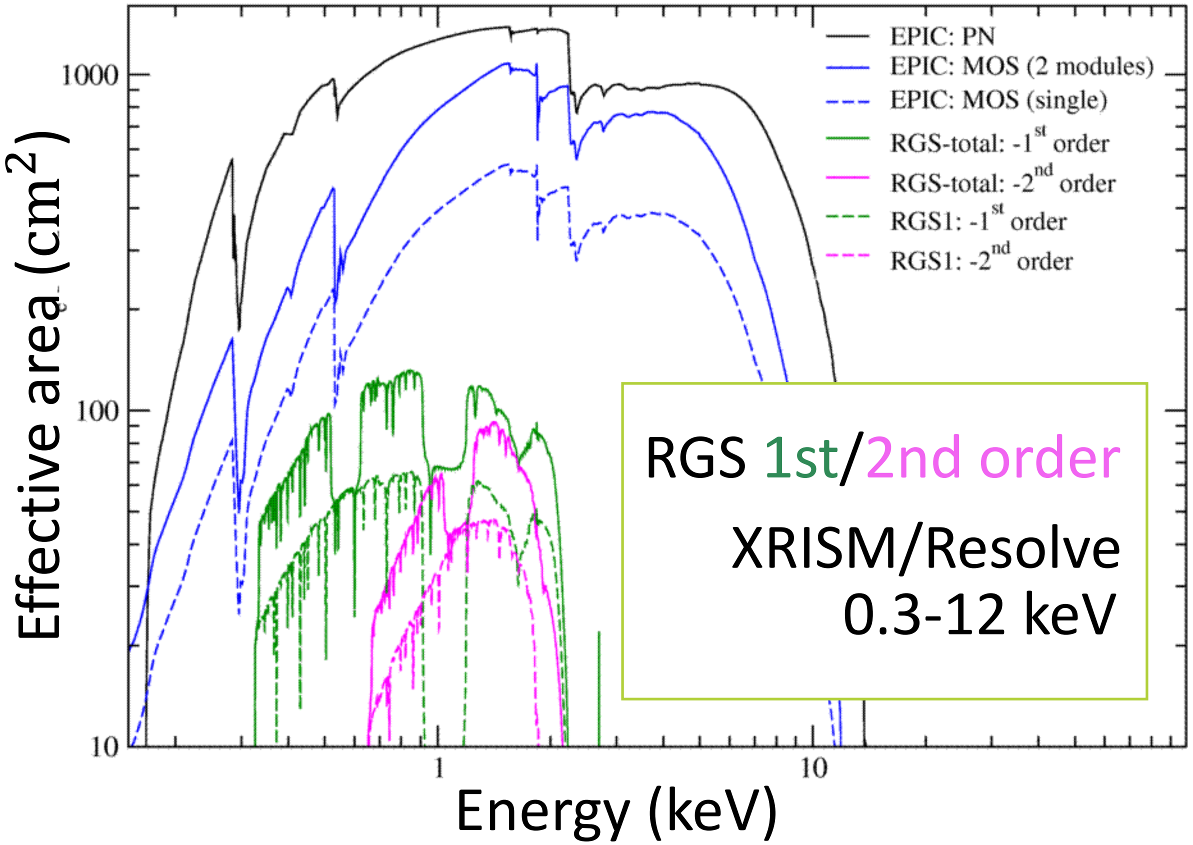

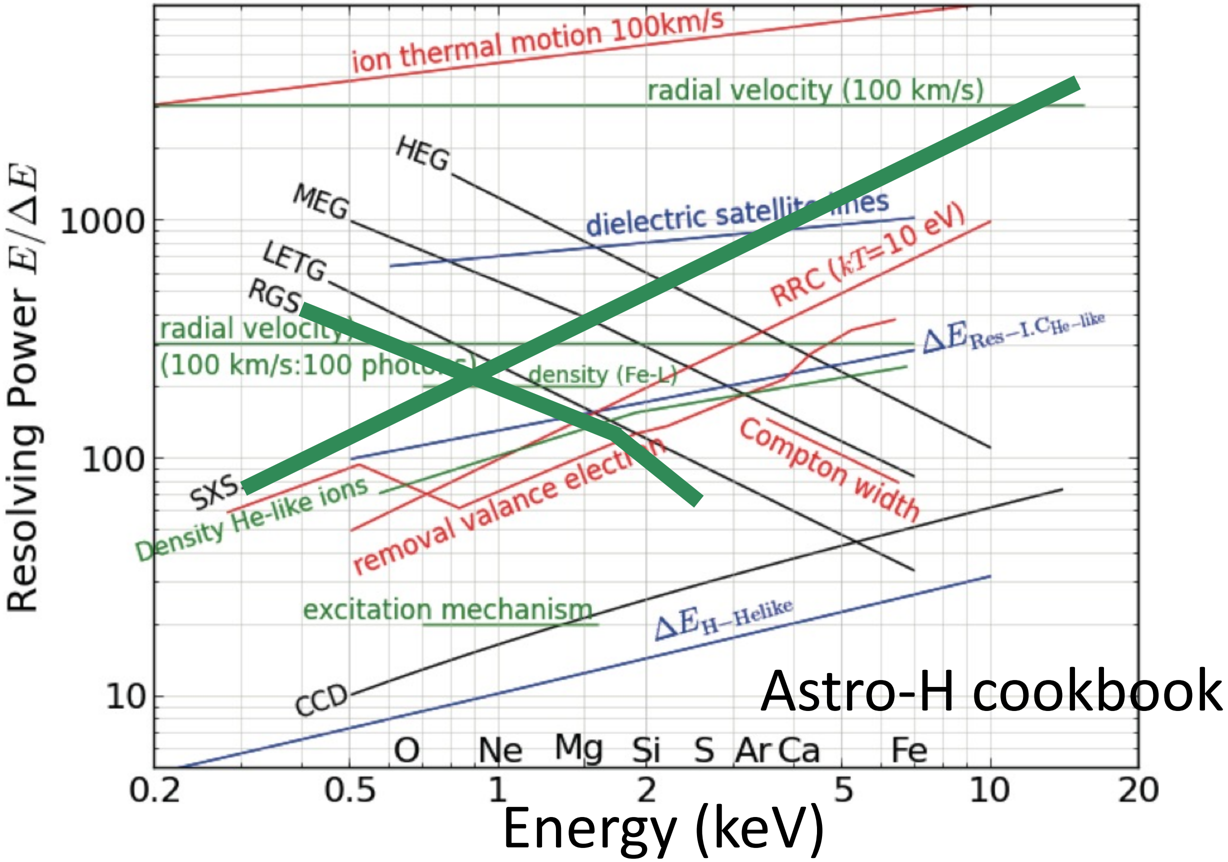

Combination of XRISM/Resolve and XMM-Newton/RGS

→ high resolution spectroscopy over a wide energy band.

Detector

✓ XMM-Newton Reflection Grating Spectrometer (RGS)
energy range: 5-38 Å (0.35-2.5 keV)

Emission lines are broadened by

$$\Delta\lambda = 0.138 \frac{\Delta\theta}{m} \text{Å}$$

$\Delta\theta$: spatial extent of the source
m : spectral order

RGS spectrum can be spatially resolved in the direction of cross dispersion angle.

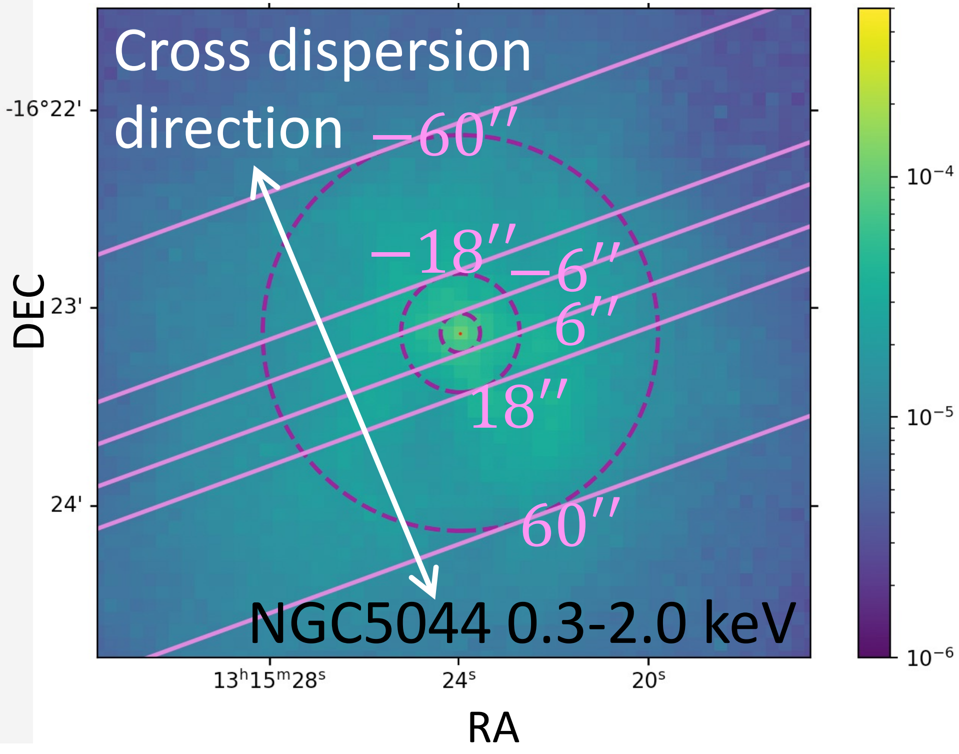

Combination of XRISM/Resolve and XMM-Newton/RGS
→broad band spectroscopy, spatial distribution of temperature and abundance profile

Target objects

NGC5044

- ✓ Nearby bright group with cool core
- ✓ ICM ~ 1 keV
- ✓ X-ray cavities
- ✓ asymmetric temperature structure

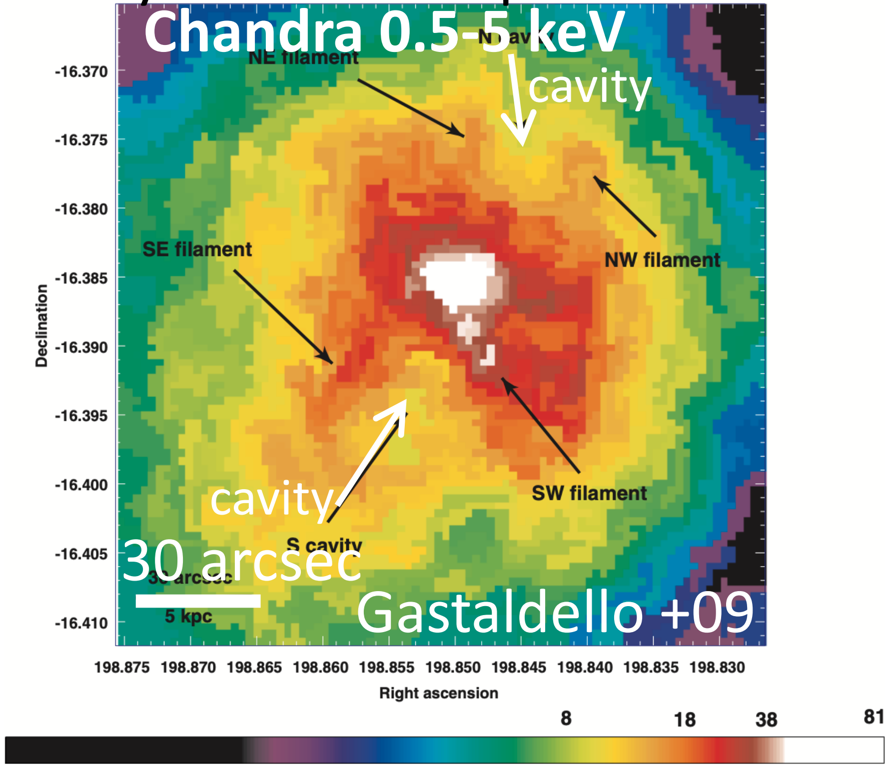

Abell 262

- ✓ Nearby bright cluster with cool core
- ✓ ICM ~ 2 keV
- ✓ X-ray cavities
- ✓ Relation between AGN activity and X-ray emission

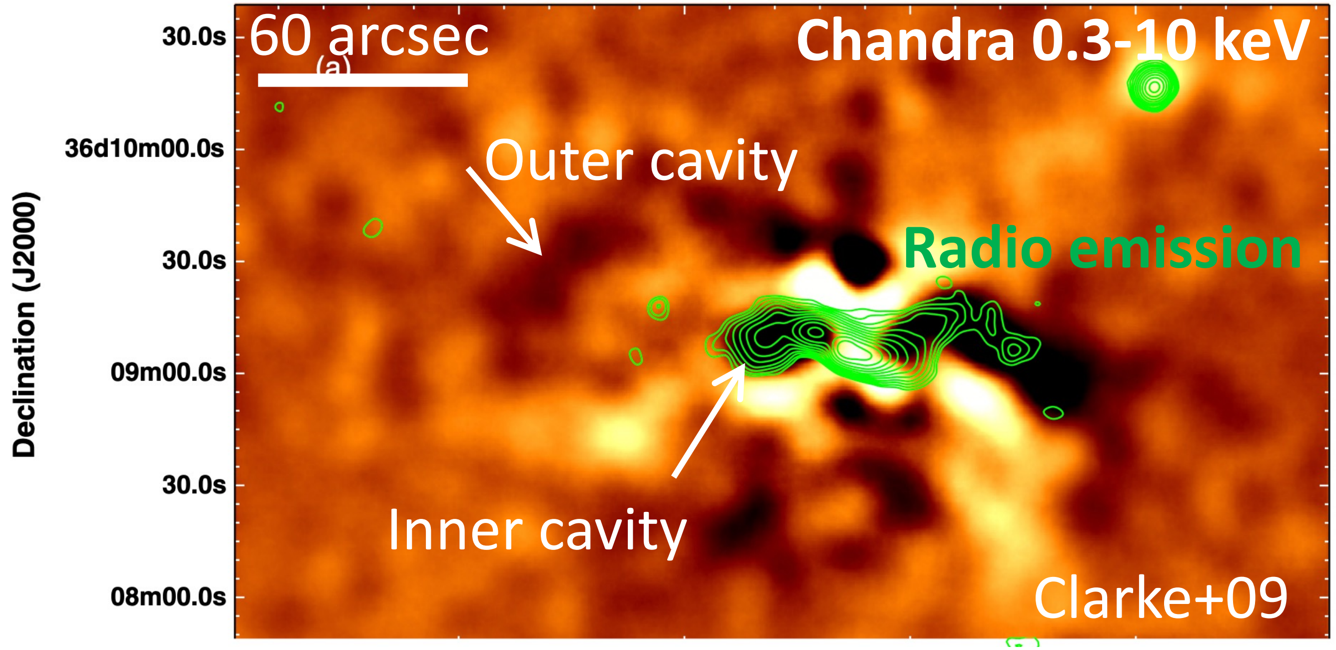

By using RGS spectrum, I tried to reveal the temperature structure and abundance ratio along the cross dispersion direction.

Spectrum of NGC5044 central region (−6″~6″)

phabs*(**rgsxsrc***bvvapec$_{\mathrm{high\ kT}}$ + **gsmooth***bvvapec$_{\mathrm{low\ kT}}$)

Line broadening of High kT component

Line broadening of low kT component

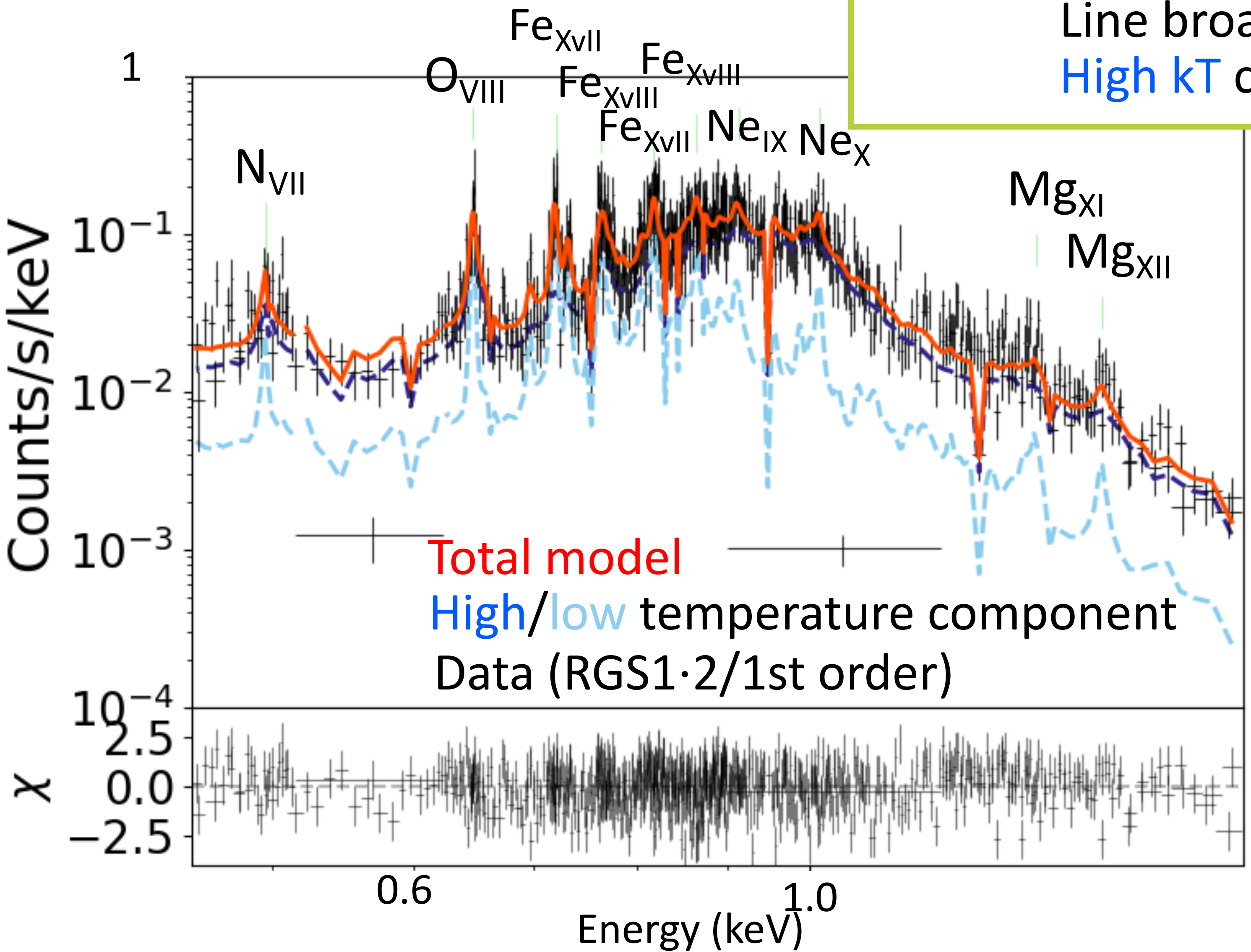

velocity broadening (km/s) = 172 (fix)

Ogorzalek+17

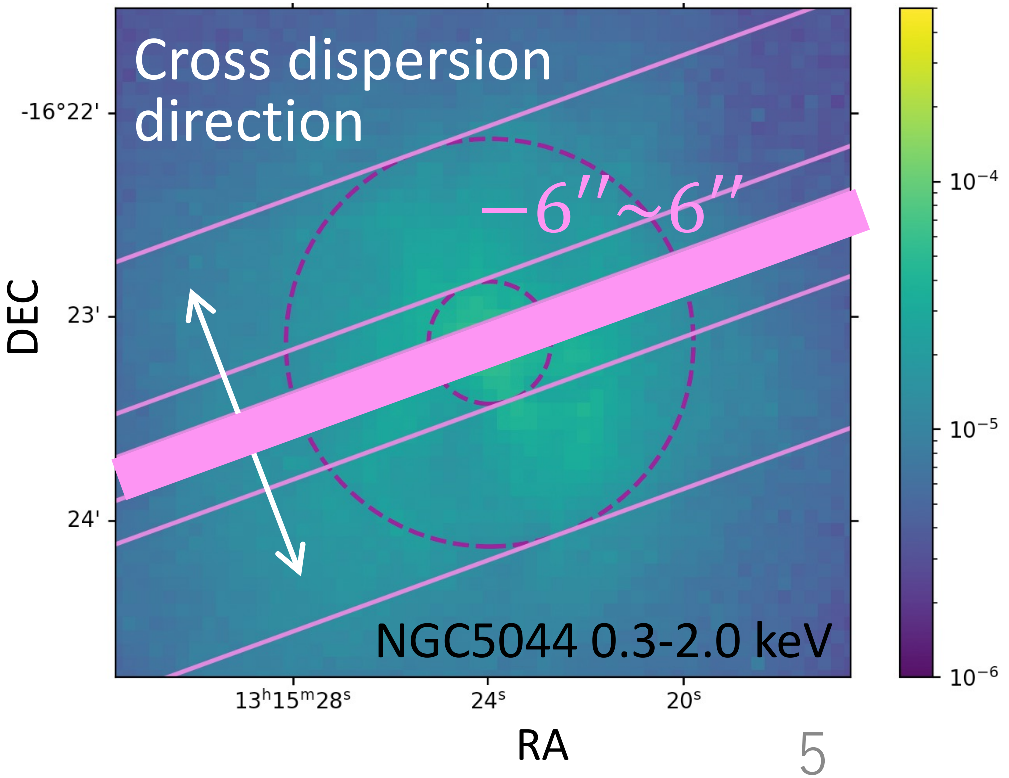

Spectrum of NGC5044 central region (−6″~6″)

phabs*(**rgsxsrc***bvvapec$_{\text{high kT}}$ + **gsmooth***bvvapec$_{\text{low kT}}$)

Line broadening of High kT component

Line broadening of low kT component

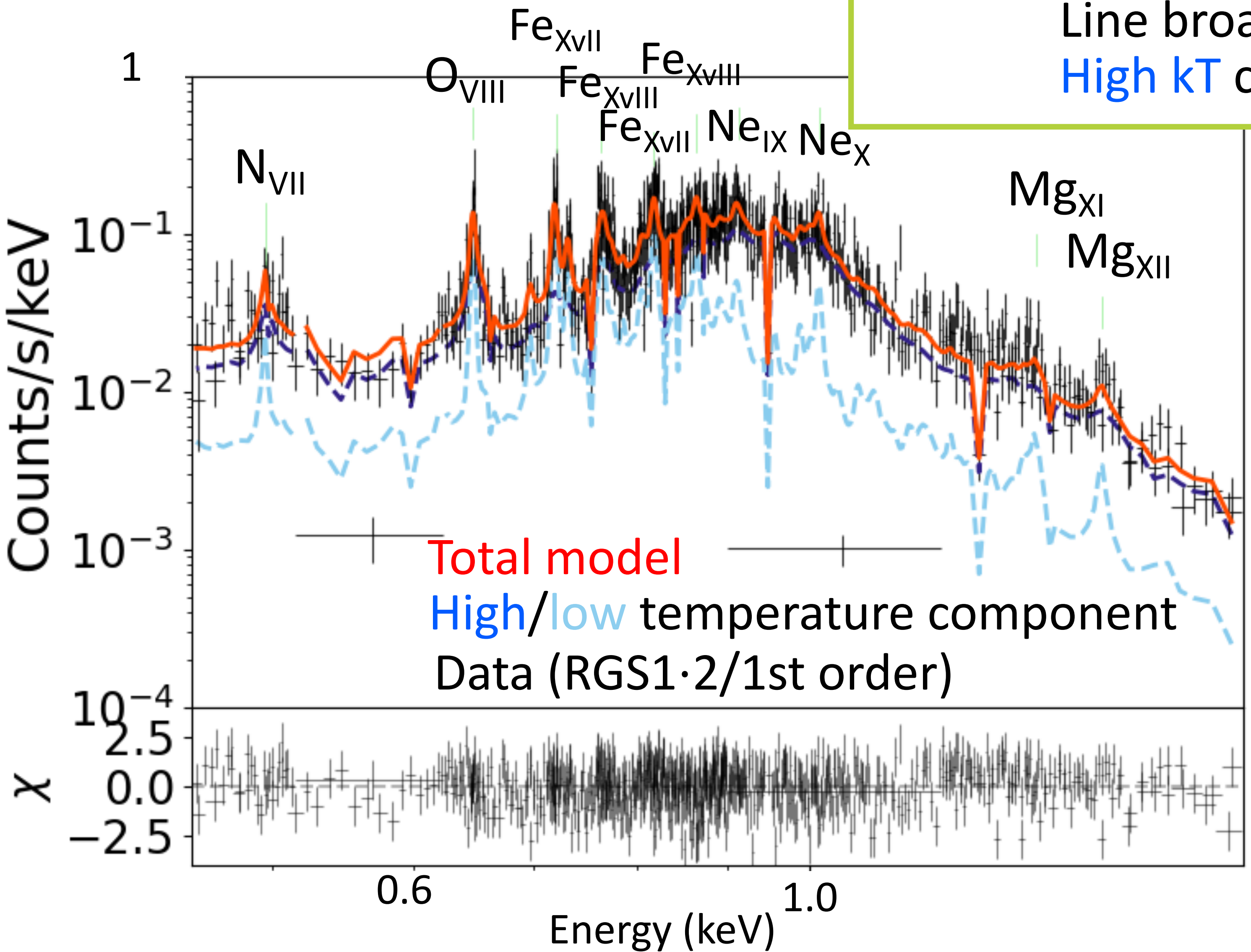

velocity broadening (km/s) = 172 (fix)

Ogorzalek+17

rgsxsrc model

- ✓ Convolve RGS spectrum for extended emission
- ✓ I use an image (**0.7-2.0** keV)

gsmooth model

- ✓ Gaussian smoothing

Spectrum of NGC5044 central region (−6″~6″)

phabs*(**rgsxsrc***bvvapec$_{\text{high kT}}$ + **gsmooth***bvvapec$_{\text{low kT}}$)

Line broadening of High kT component

Line broadening of low kT component

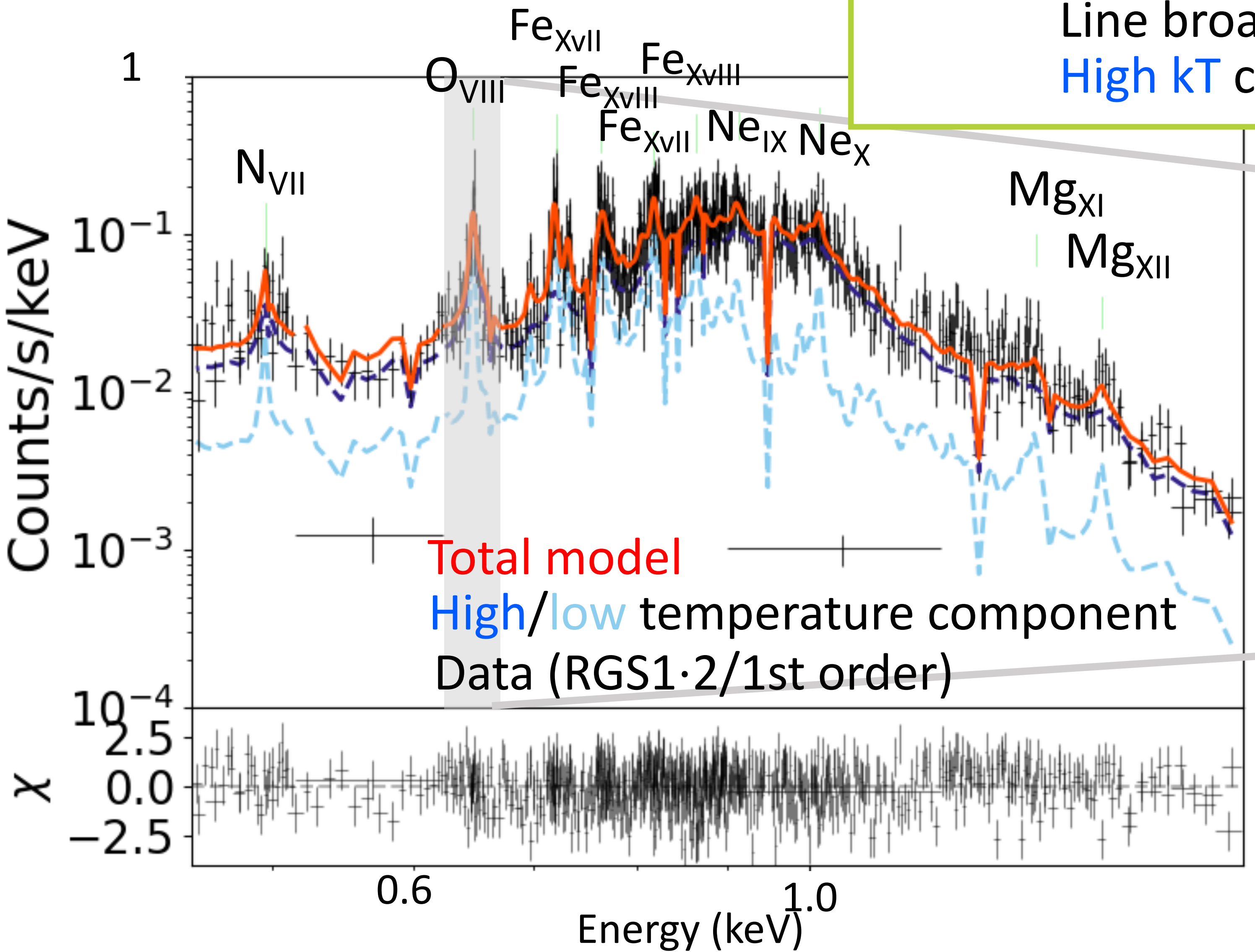

velocity broadening (km/s) = 172 (fix)

Ogorzalek+17

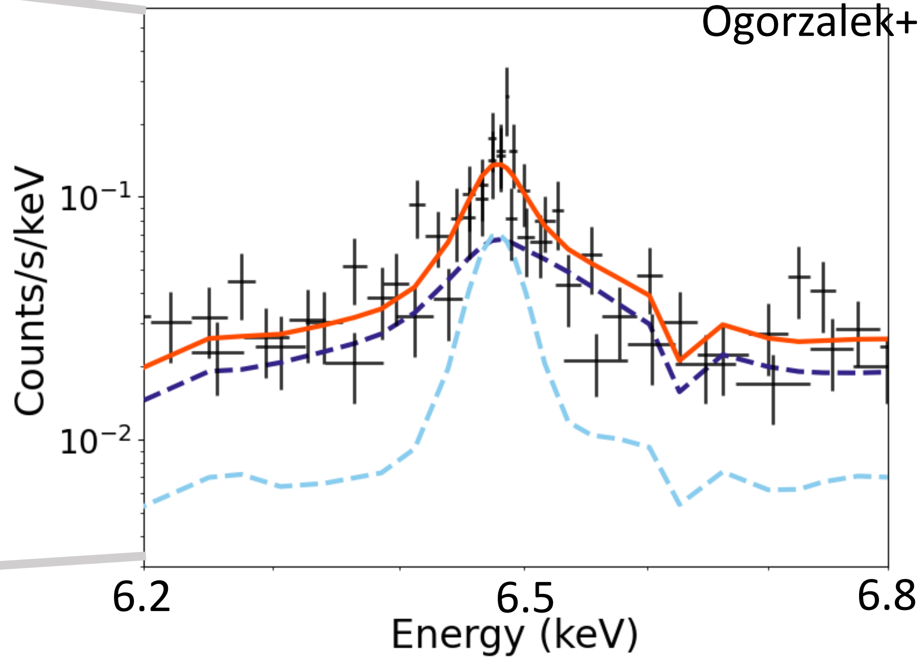

In −6″~6″ region,
higher kT component has a more diffuse distribution than lower one.

Temperature

NGC5044

phabs*(rgsxsrc*$\text{bvvapec}_{\text{high kT}}$ + gsmooth*$\text{bvvapec}_{\text{low kT}}$)

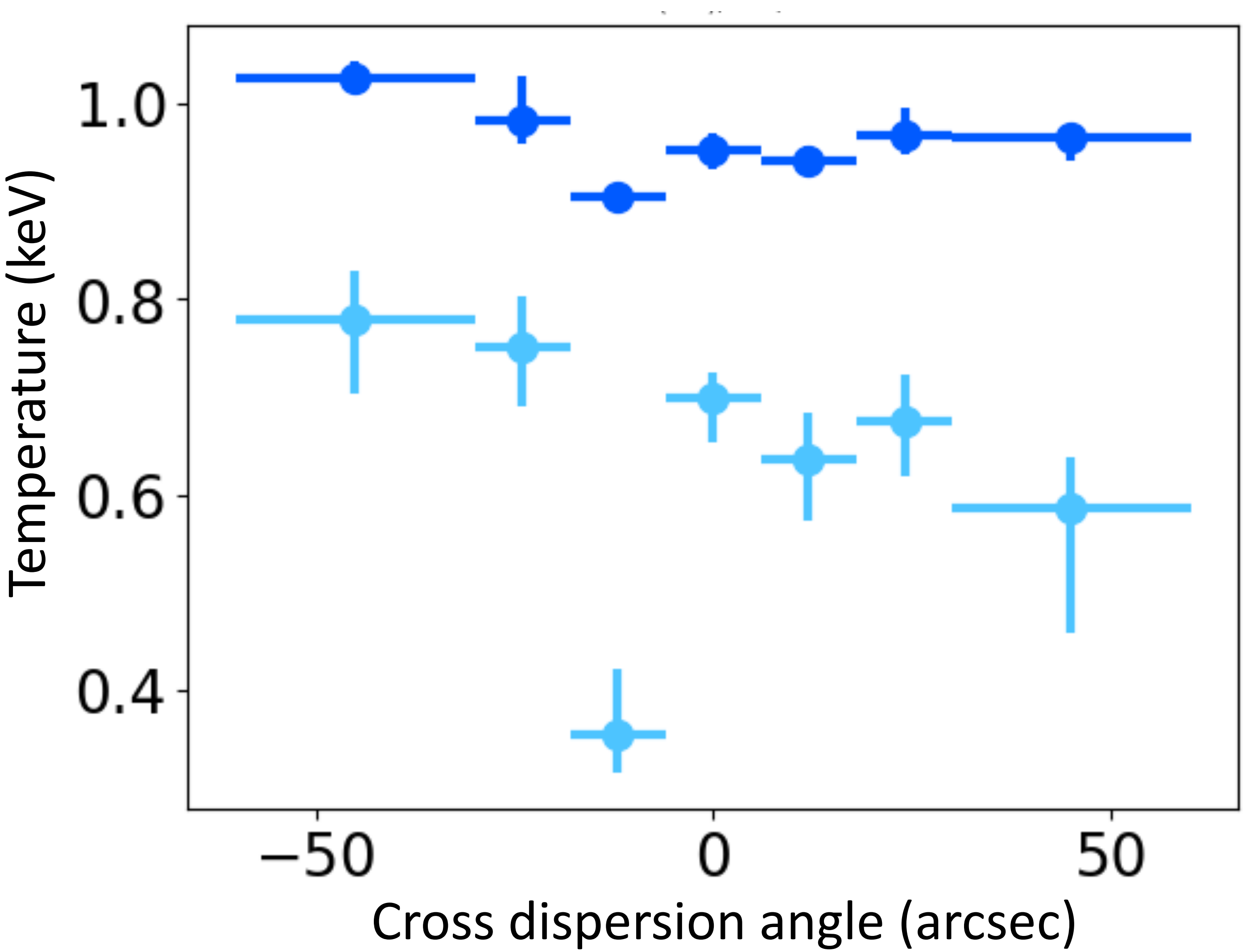

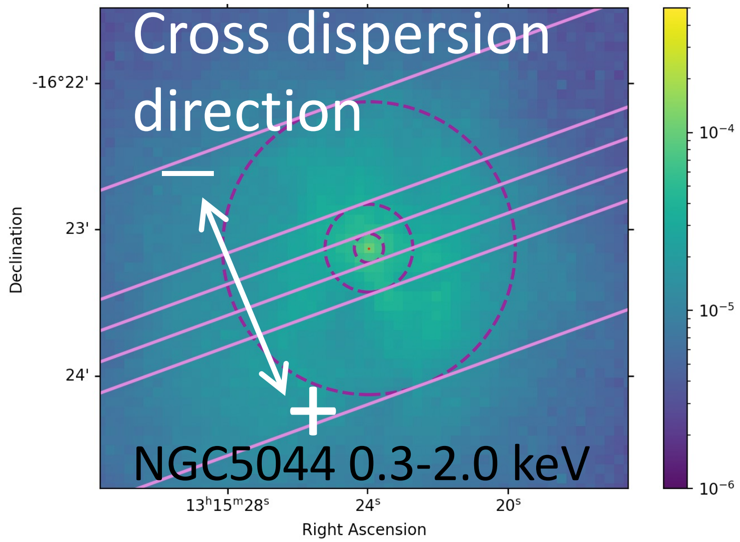

✓ 0.6 ~ 0.8 keV plasma exists in the central region.

✓ $\dfrac{\text{Norm}_{\text{low kT}}}{\text{Norm}_{\text{high kT}}}$ ~ 10-50%

O/Fe Abundance

NGC5044

phabs*(rgsxsrc*bvvapec$_{\text{high kT}}$ + gsmooth*bvvapec$_{\text{low kT}}$)

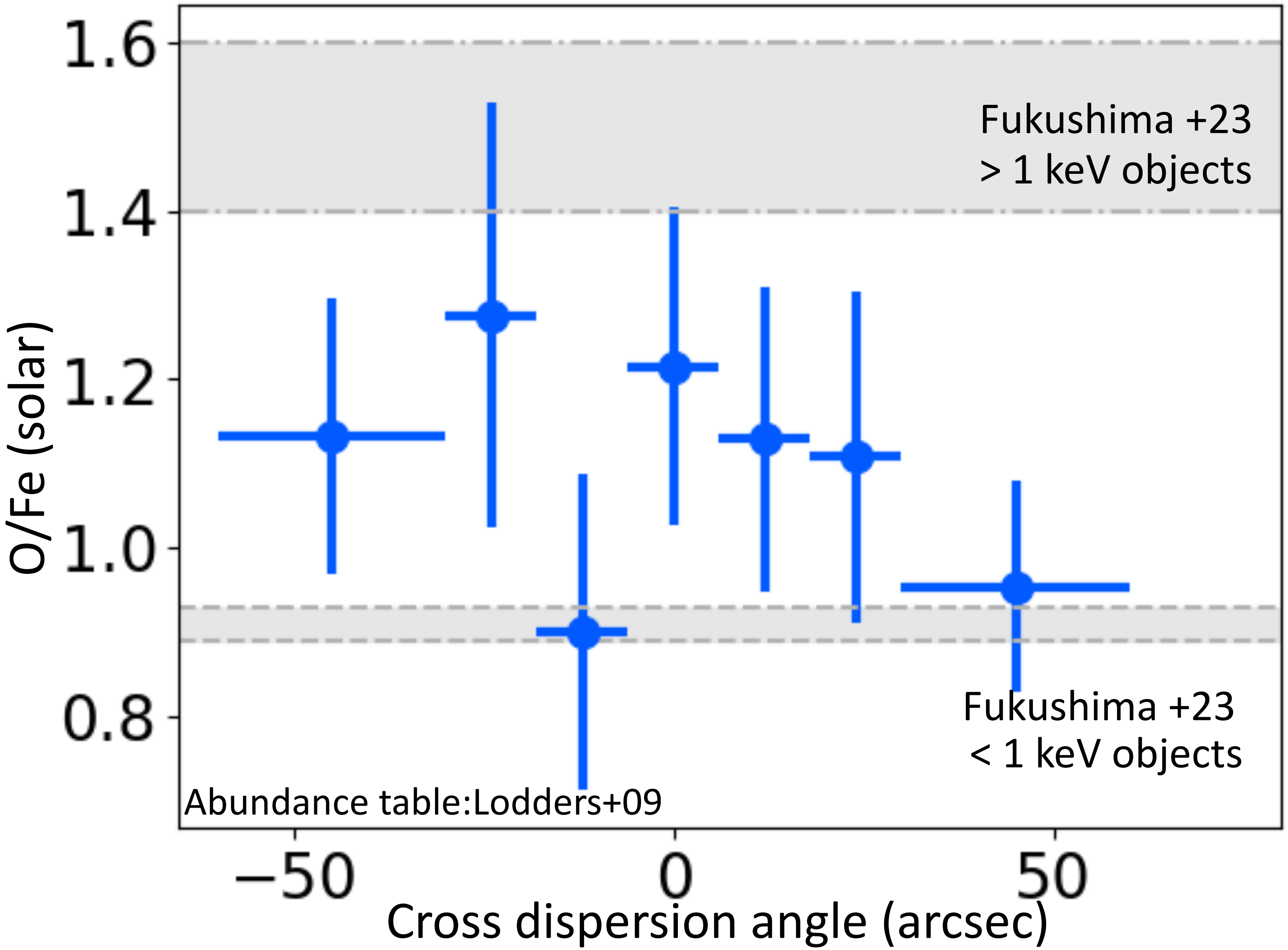

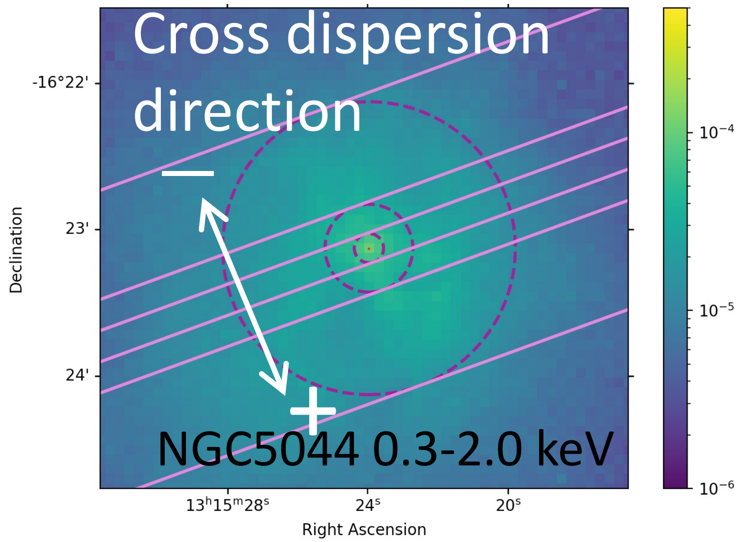

- ✓ O/Fe ~ Solar
- ✓ No major discrepancy with previous study

O/Fe Abundance XSPEC vs SPEX

NGC5044

XSPEC phabs*(rgsxsrc*bvvapec$_{\mathrm{high\ kT}}$ + gsmooth*bvvapec$_{\mathrm{low\ kT}}$)

SPEX hot*lpro*(cie + cie)

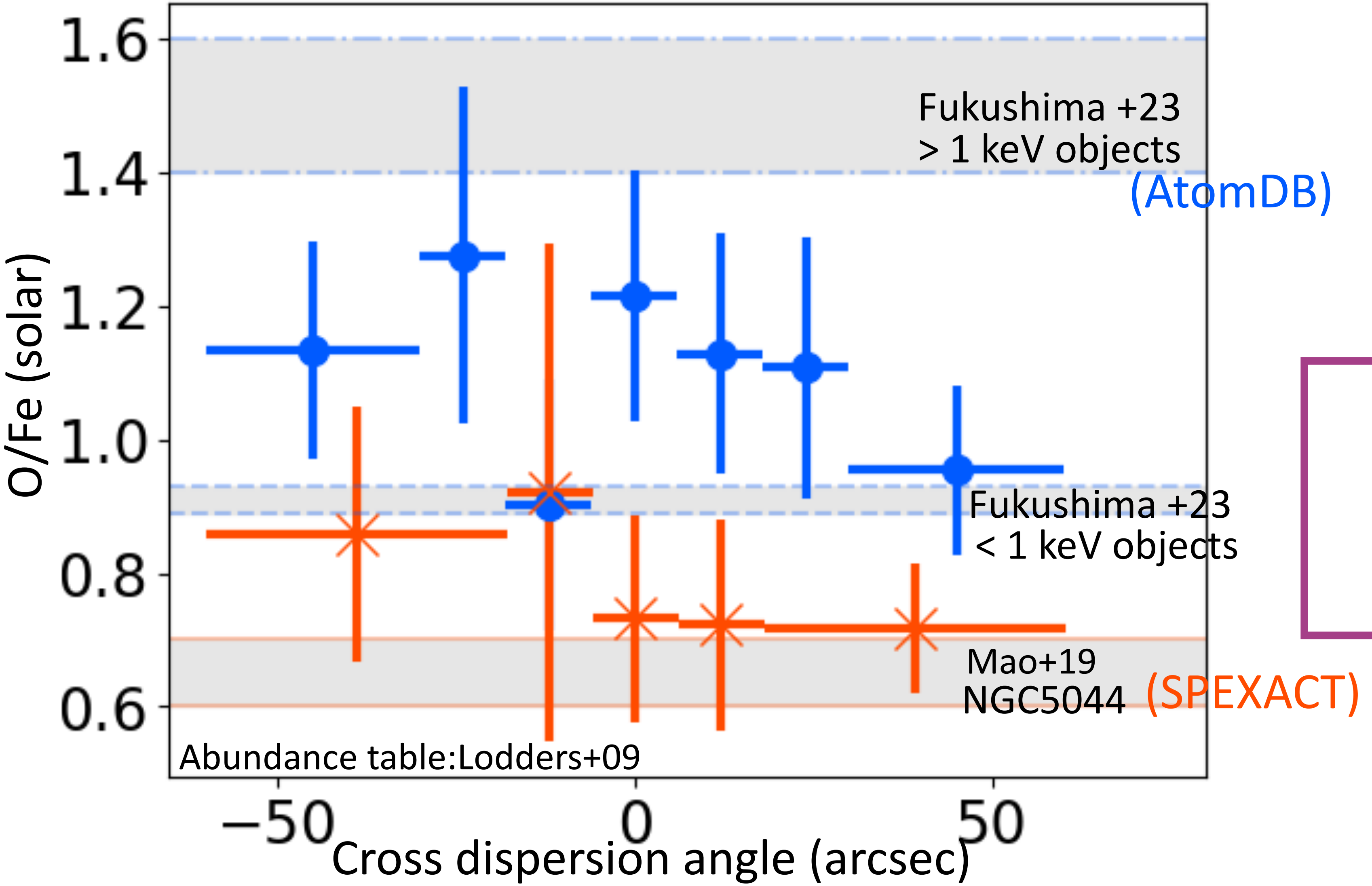

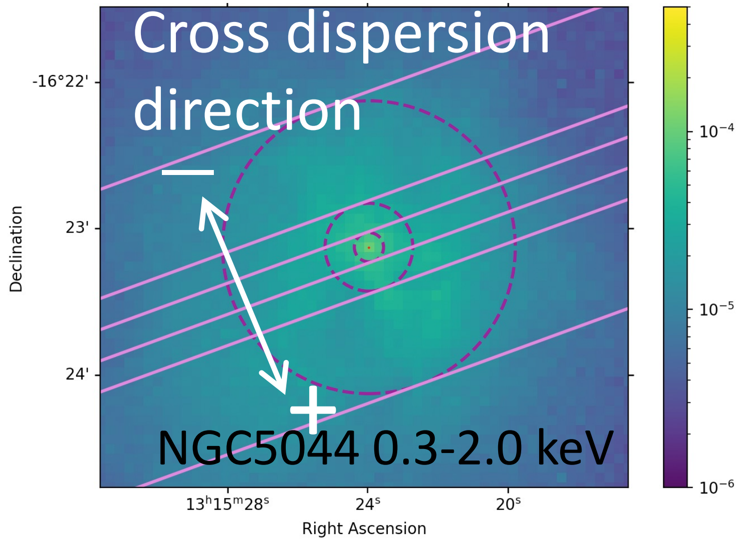

XSPEC (AtomDB)

>

SPEX (SPEXACT)

Combination of XMM-Newton/RGS and XRISM/Resolve

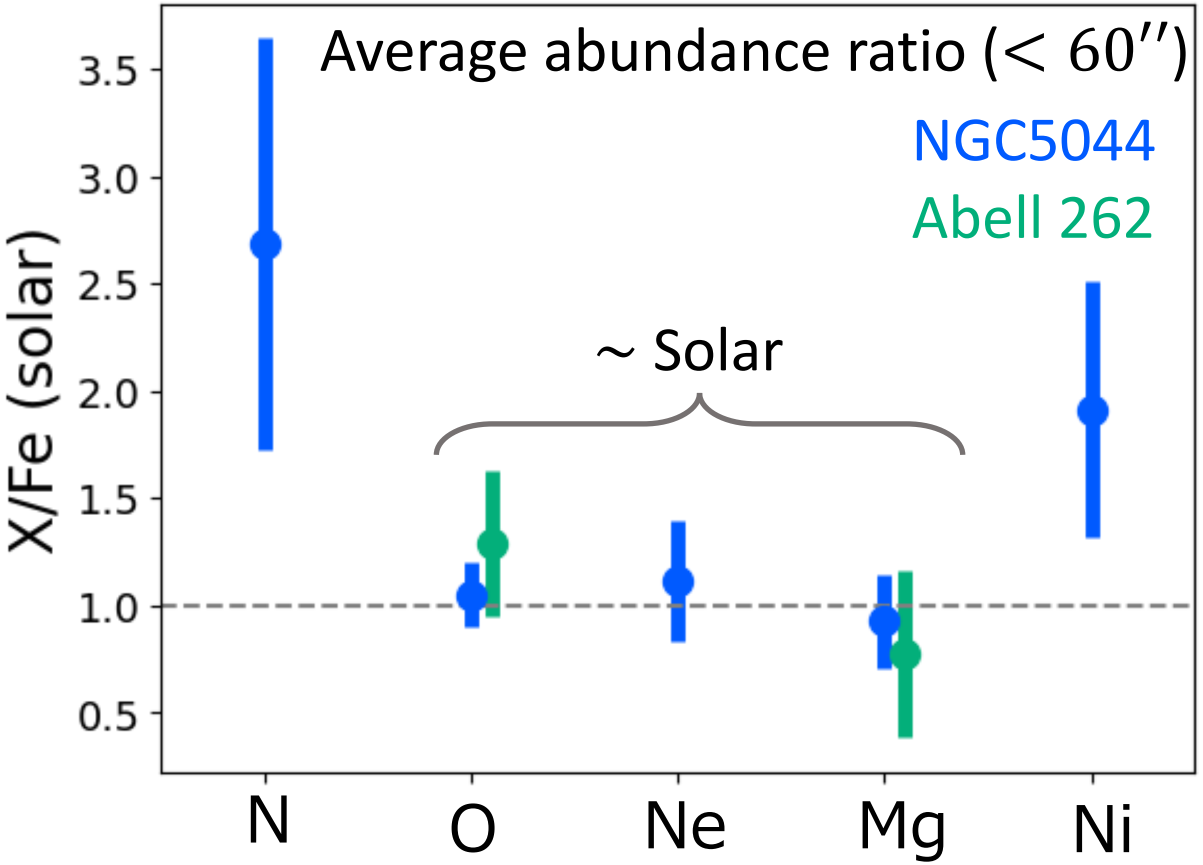

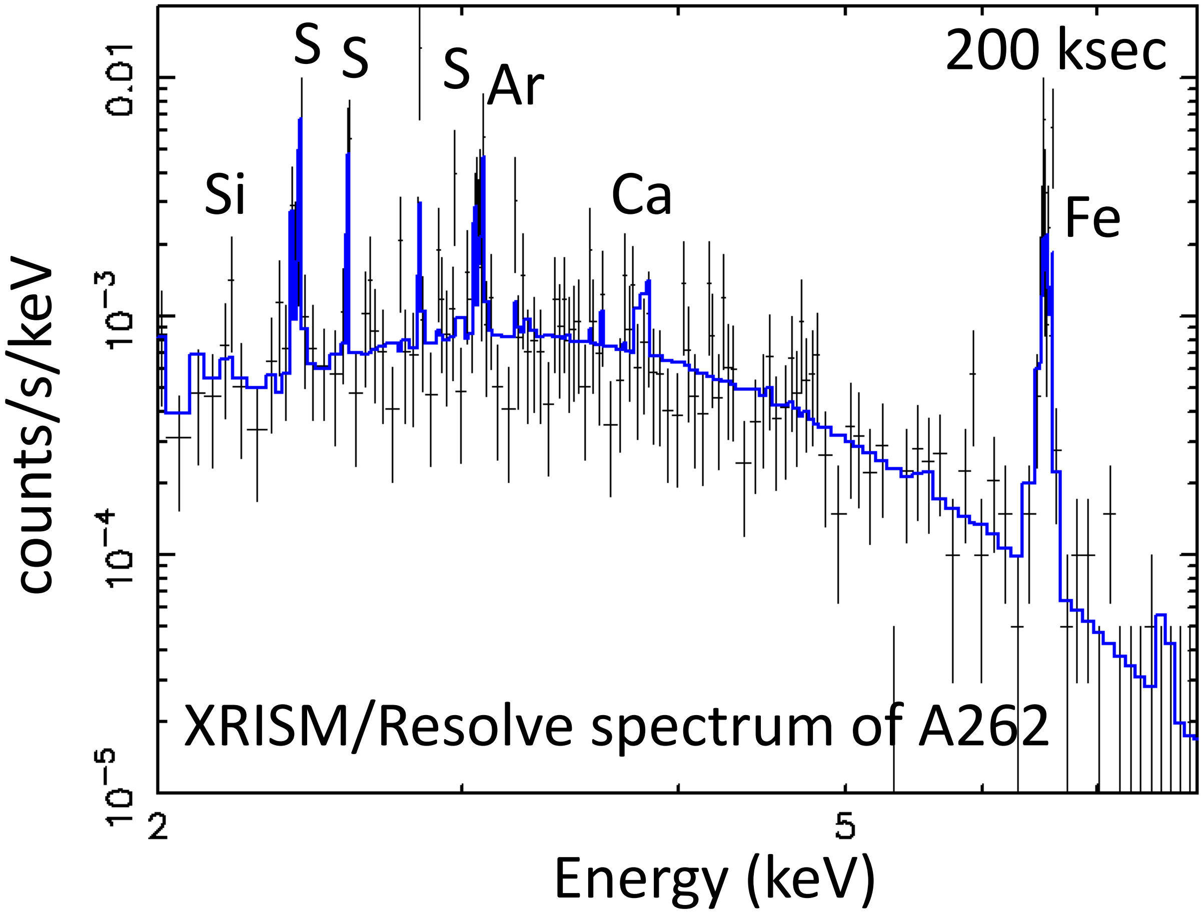

Combination of XMM-Newton/RGS (< 2 keV) and XRISM/Resolve

→ We can realize high resolution spectroscopy over a wide energy band.

backup

Spectrum of NGC5044

$\mathrm{phabs} * \mathbf{rgsxsrc} * (\mathrm{bvvapec}_{high\ kT} + \mathrm{bvvapec}_{low\ kT})$

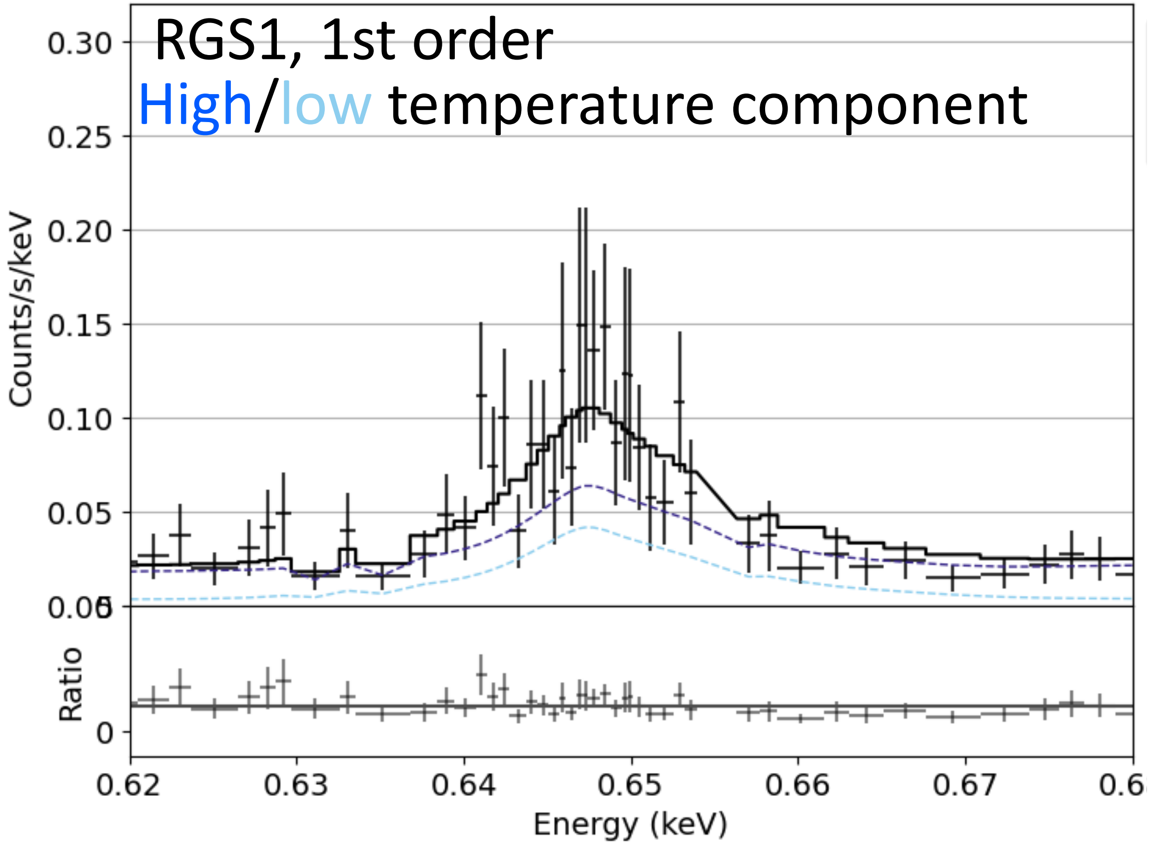

$\mathrm{phabs} * (\mathbf{rgsxsrc} * \mathrm{bvvapec}_{high\ kT} + \mathbf{gsmooth} * \mathrm{bvvapec}_{low\ kT})$

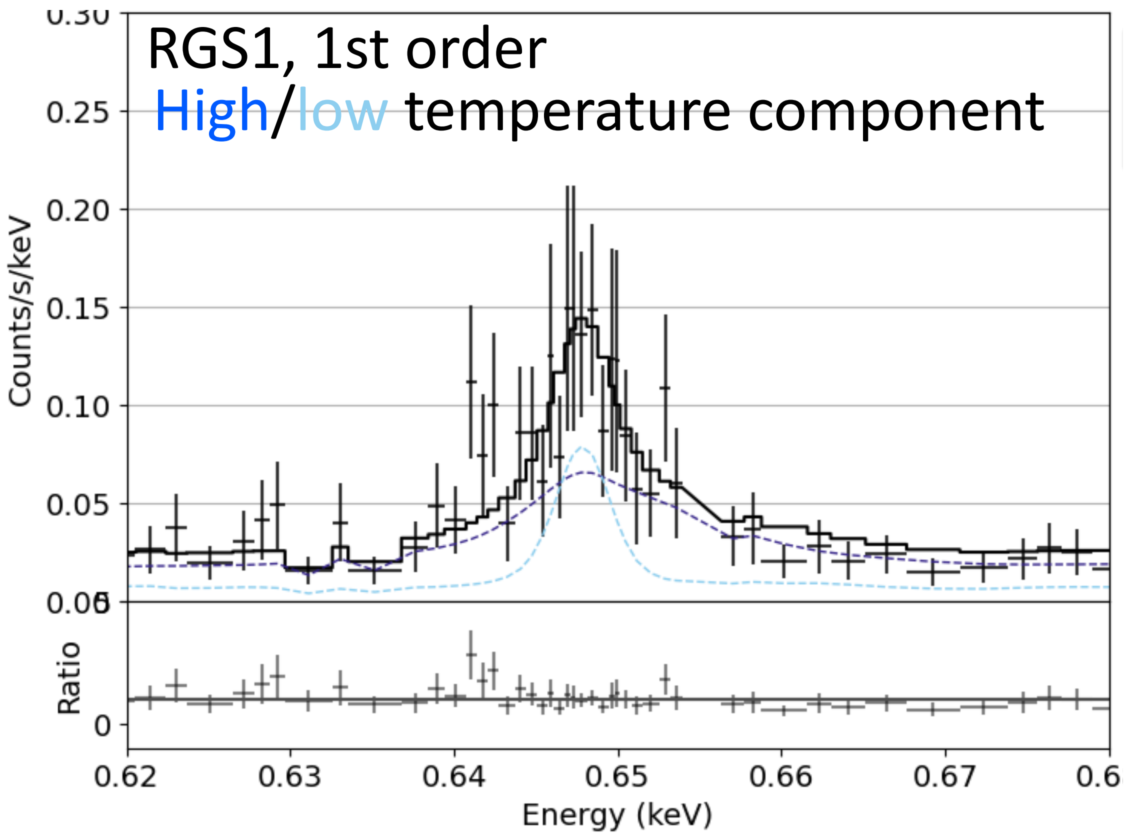

Rgsxsrc model was over-extending the O_{VIII} line of the low temperature component.

Spectrum of NGC5044

lpro*hot*(cie+cie)

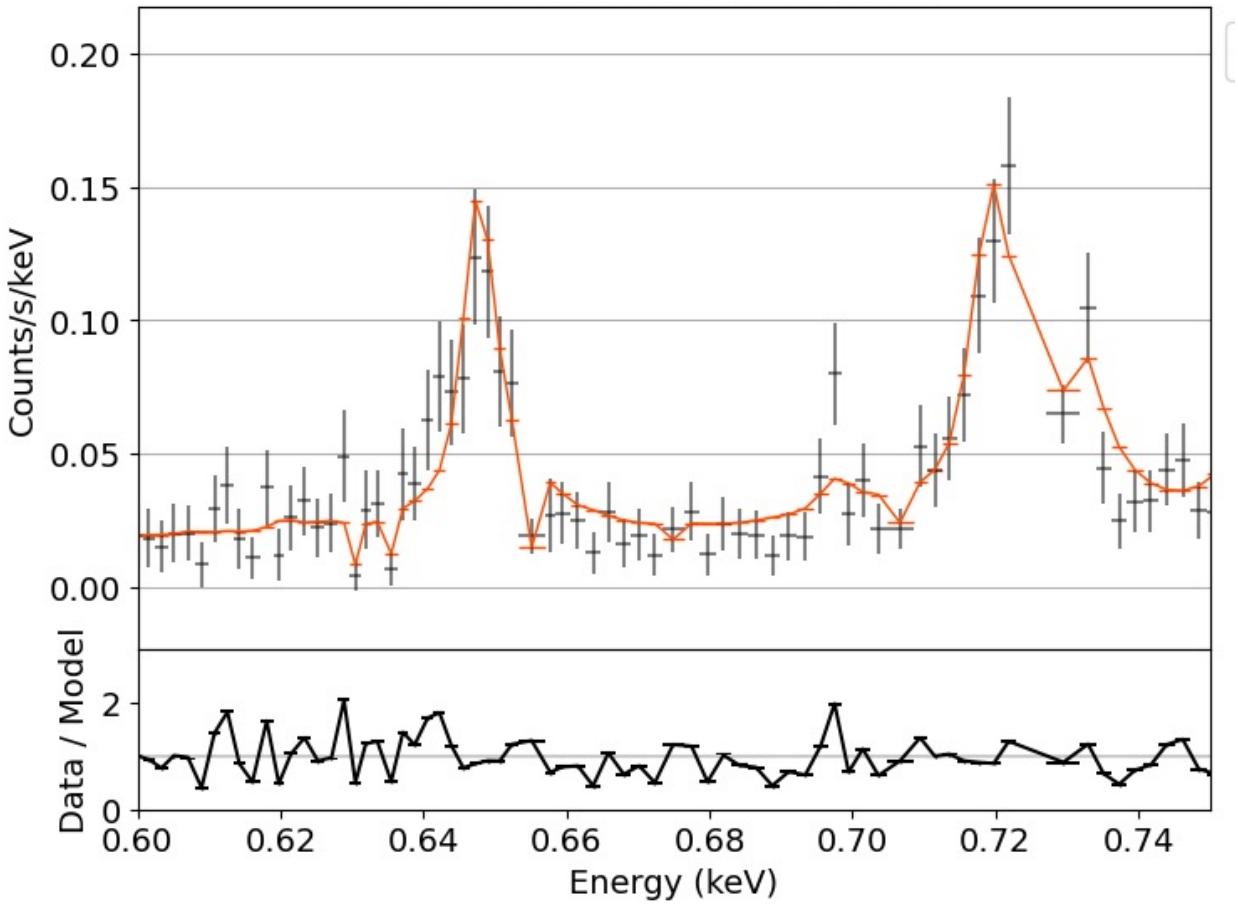

hot*(lpro*$cie_{high\ kT}$+$cie_{low\ kT}$)

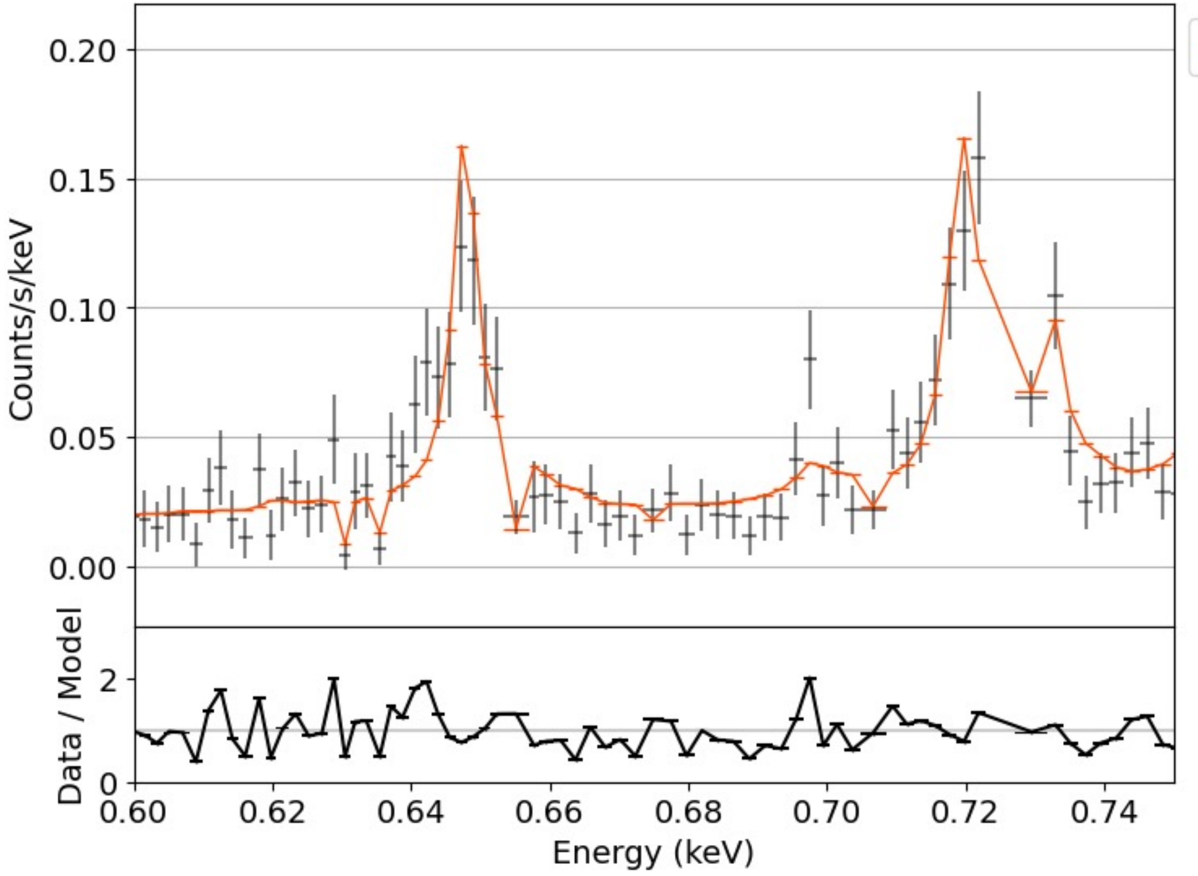

Fit results did not change significantly in SPEX.

Spectrum of NGC5044

phabs*(**rgsxsrc***bvvapec$_{\text{high kT}}$ + **gsmooth***bvvapec$_{\text{low kT}}$)

Phabs ***rgsxsrc***(bvvapec$_{\text{high kT}}$ +bvvapec$_{\text{low kT}}$)

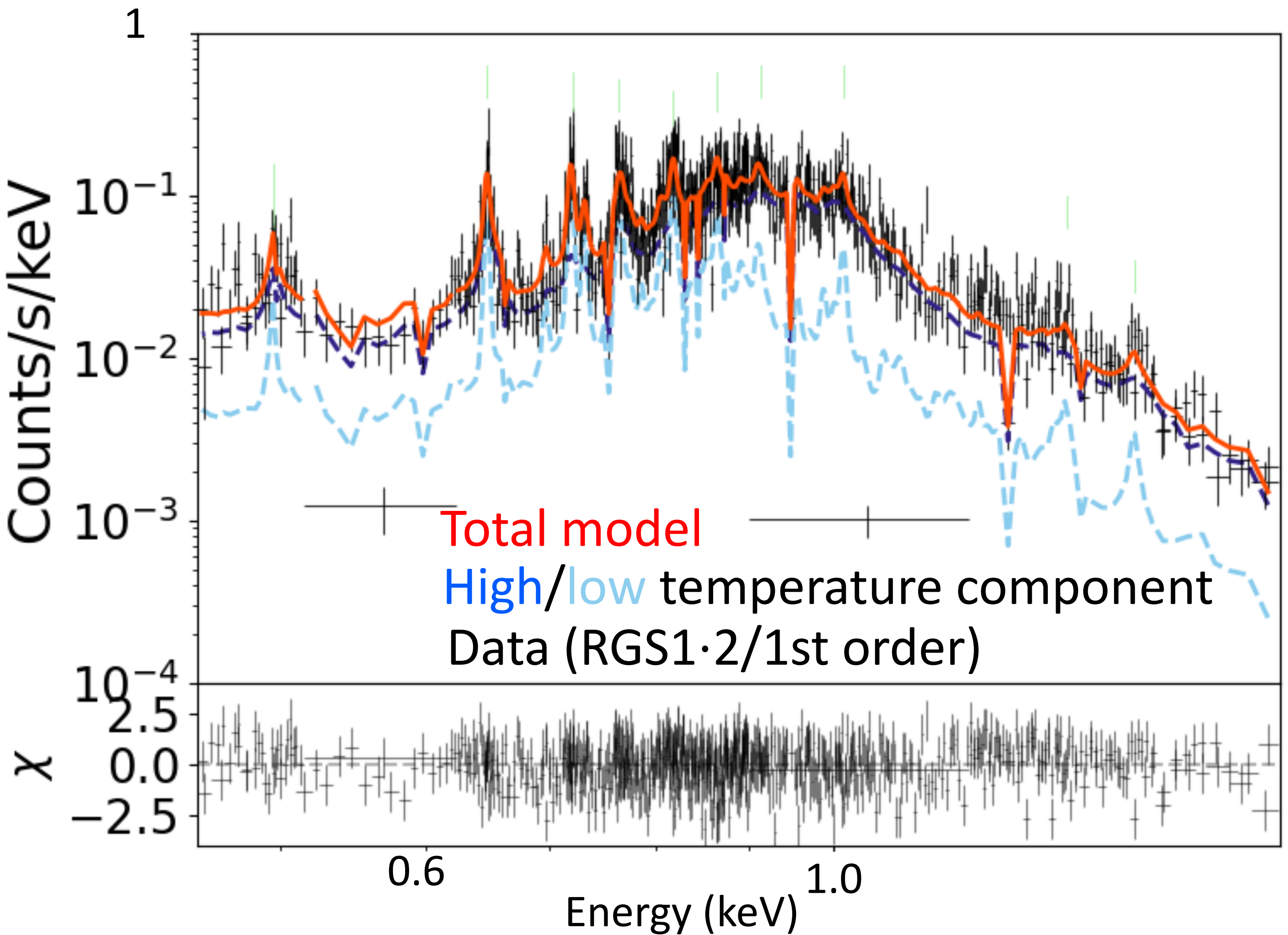

phabs*(**rgsxsrc***bvvapec$_{\text{high}}$+**gsmooth***bvvapec$_{\text{low}}$)

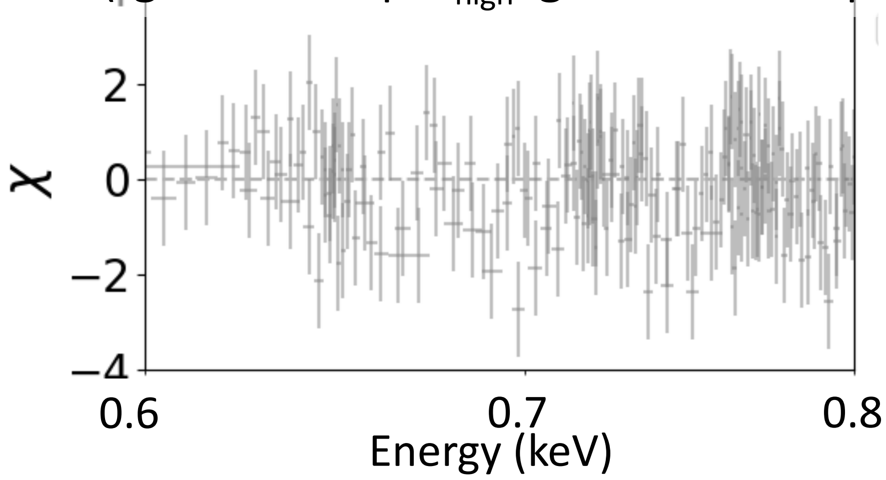

Phabs ***rgsxsrc***(bvvapec$_{\text{high kT}}$ +bvvapec$_{\text{low kT}}$)

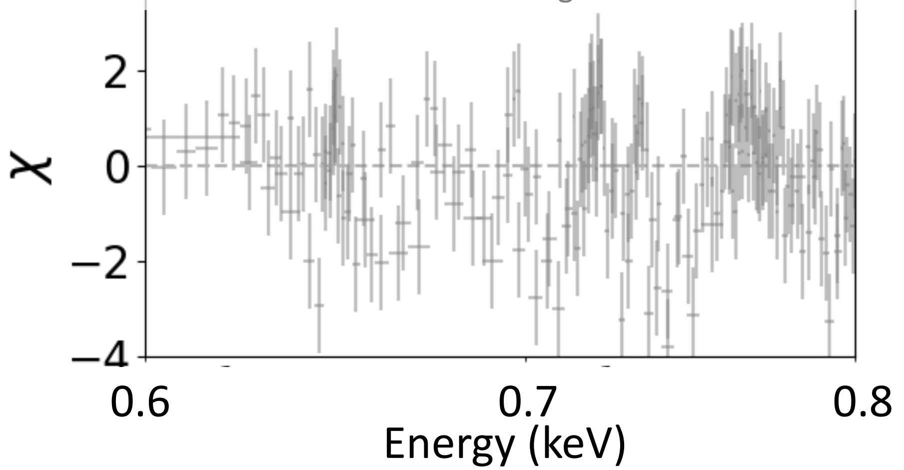

Spectrum of NGC5044

XSPEC best fit model

phabs*(**rgsxsrc***bvvapec$_{\text{high kT}}$ + **gsmooth***bvvapec$_{\text{low kT}}$)

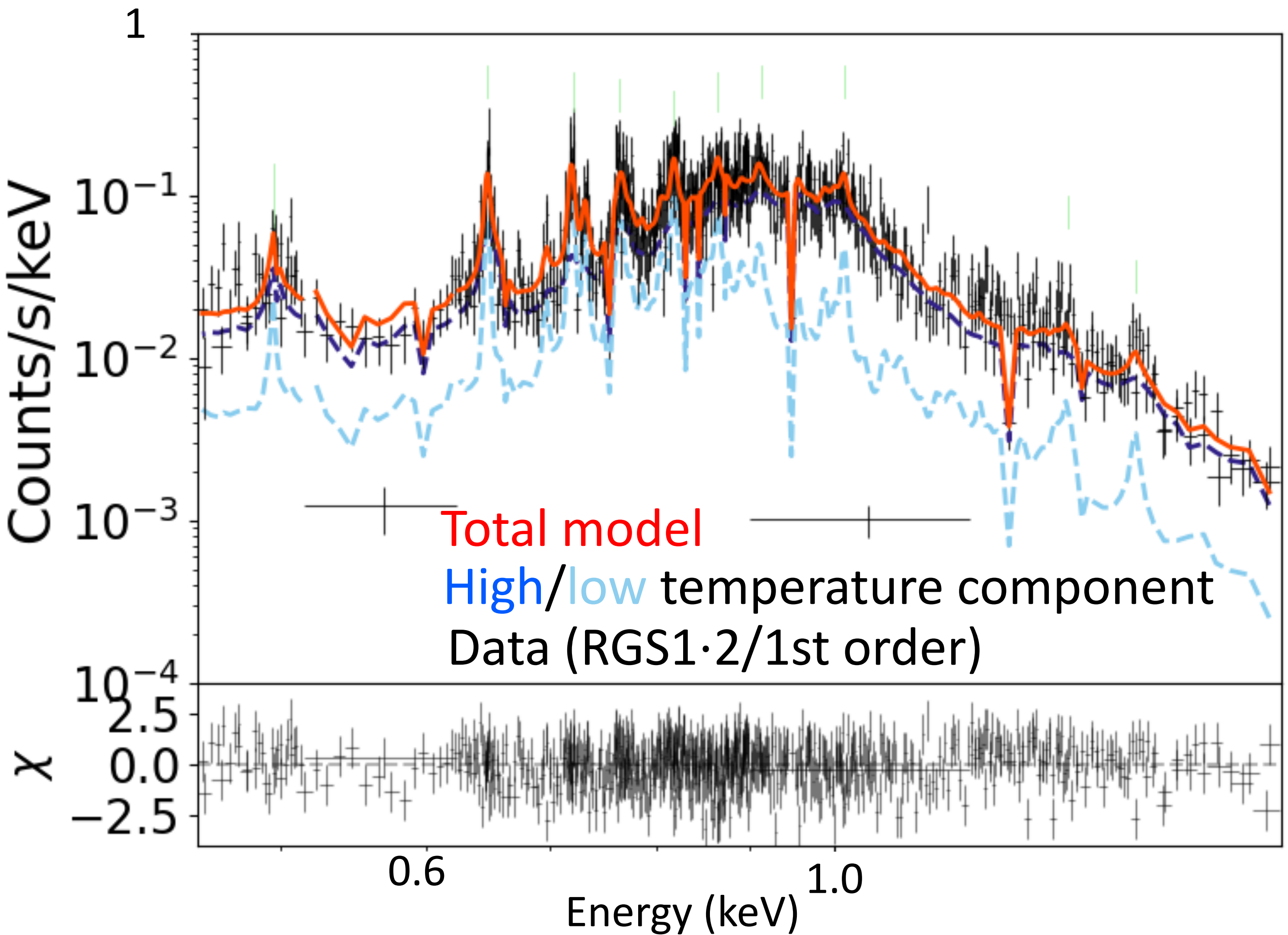

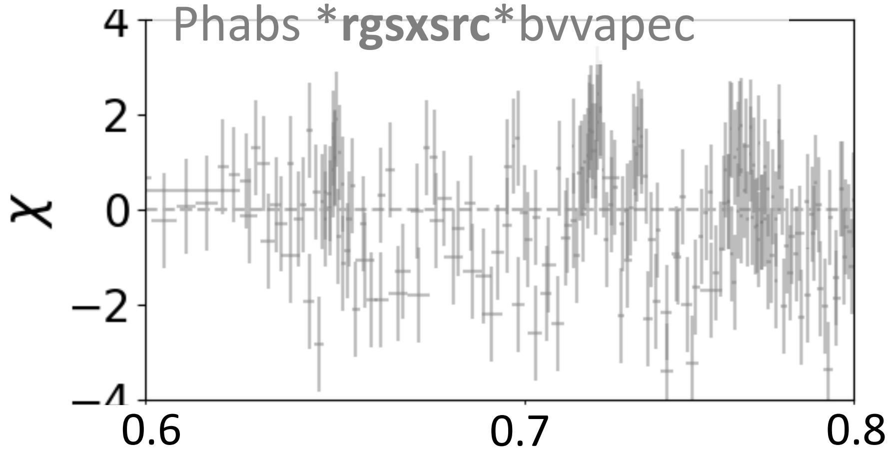

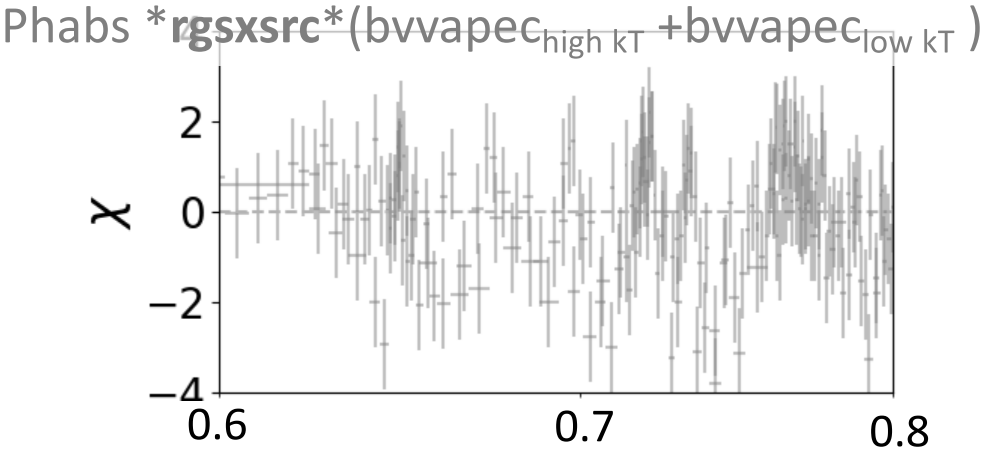

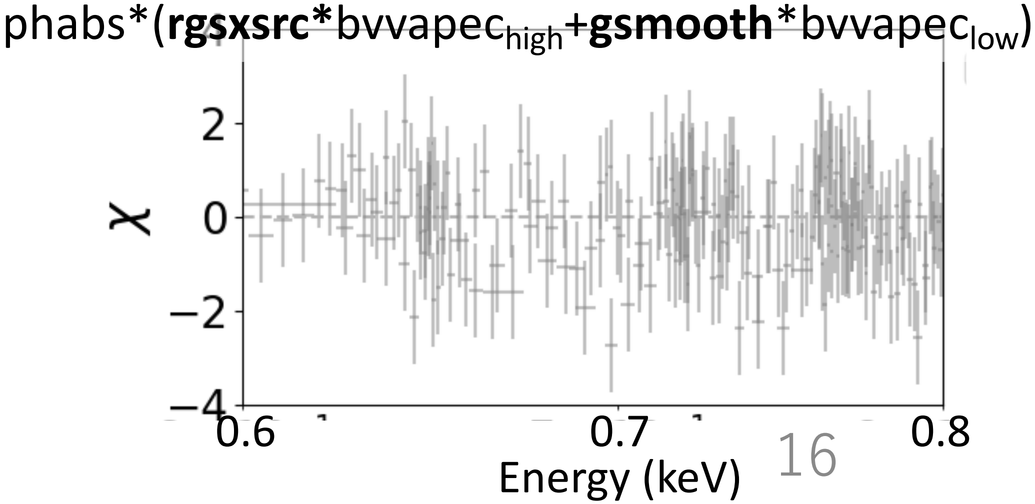

NGC5044

0.3-1.0 keV image /1.0-2.0 keV image

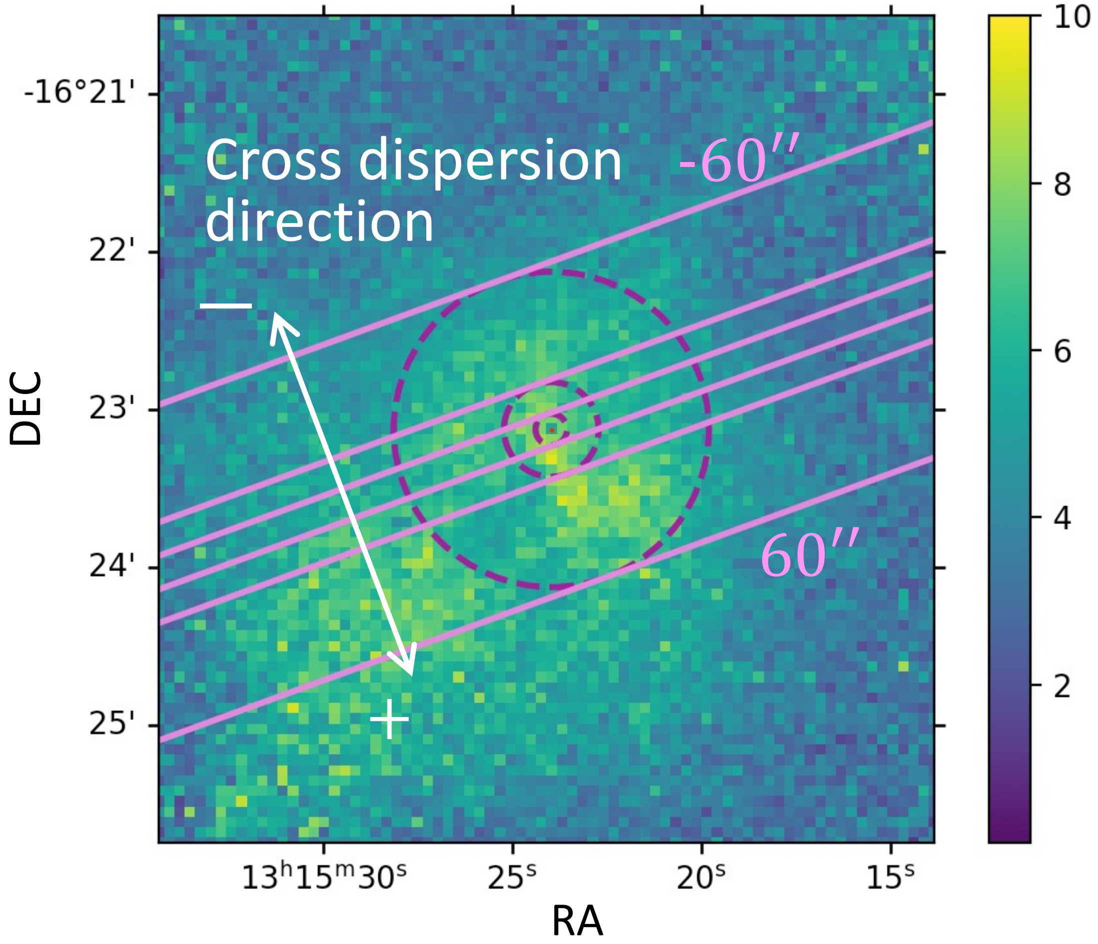

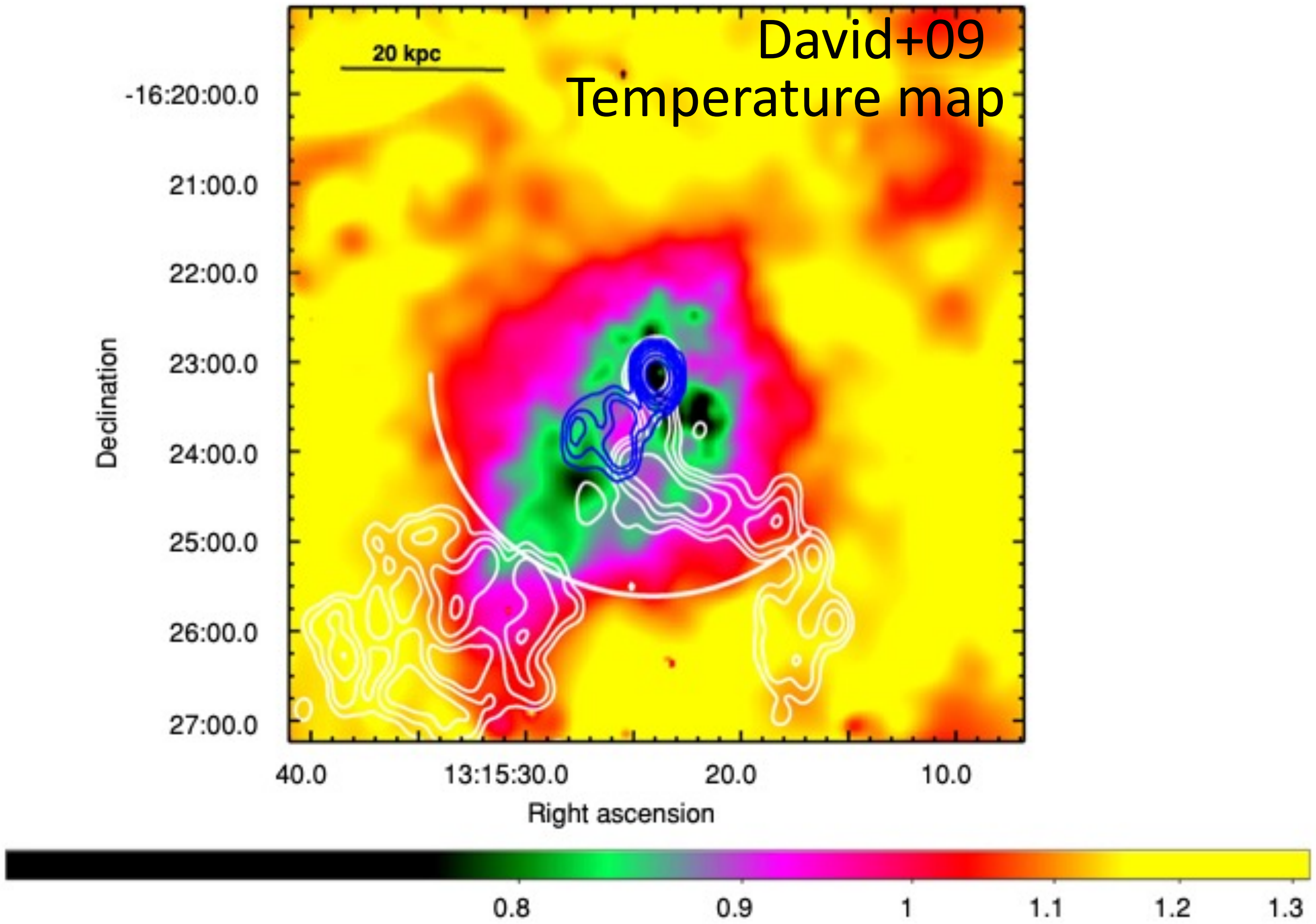

Abell 262

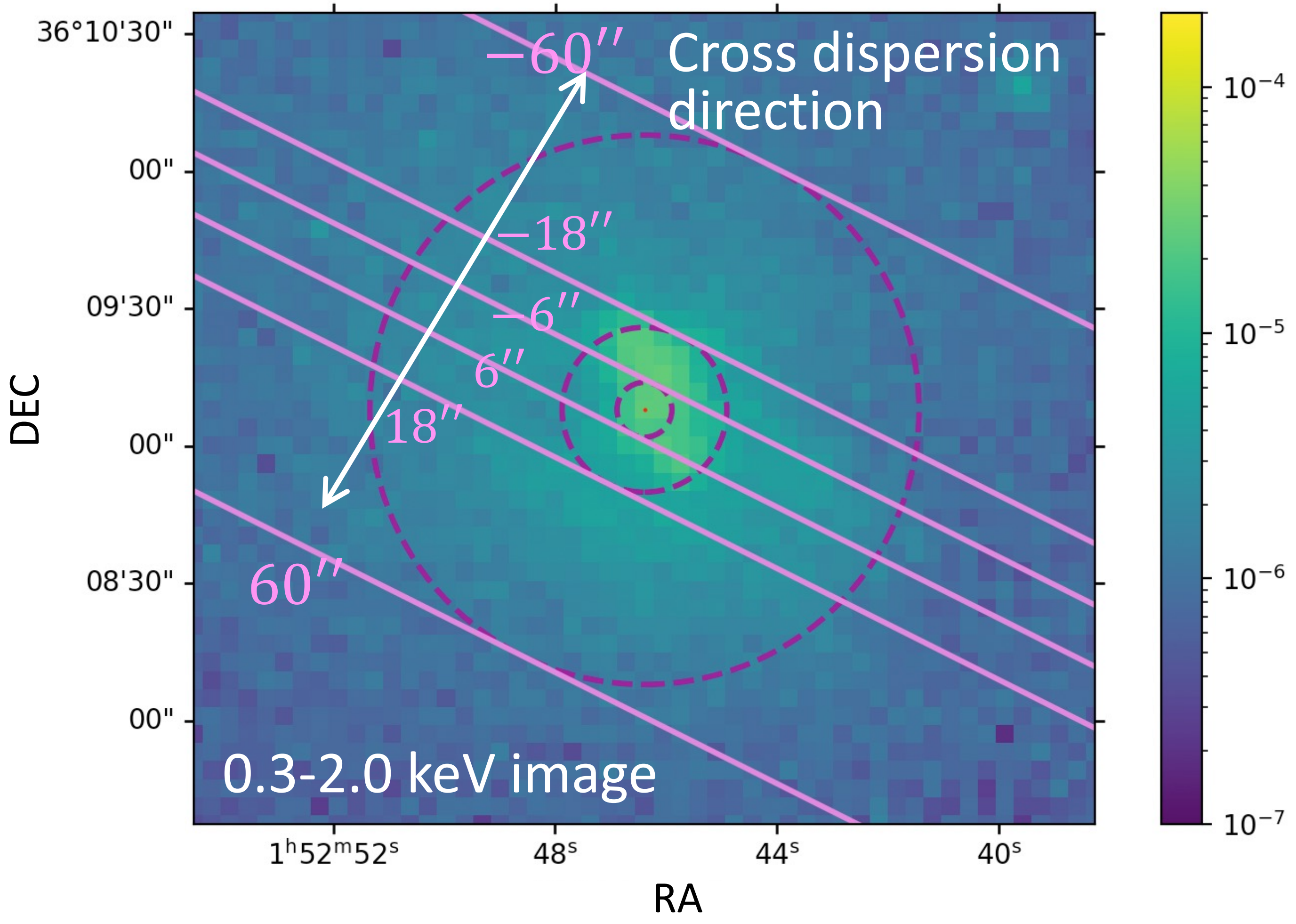

36°10'30"
00"
09'30"
00"
08'30"
00"
DEC
$1^h52^m52^s$
48^s
44^s
40^s
RA
$-60''$
$-18''$
$-6''$
$6''$
$18''$
$60''$
Cross dispersion direction
0.3-2.0 keV image
10^{-4}
10^{-5}
10^{-6}
10^{-7}

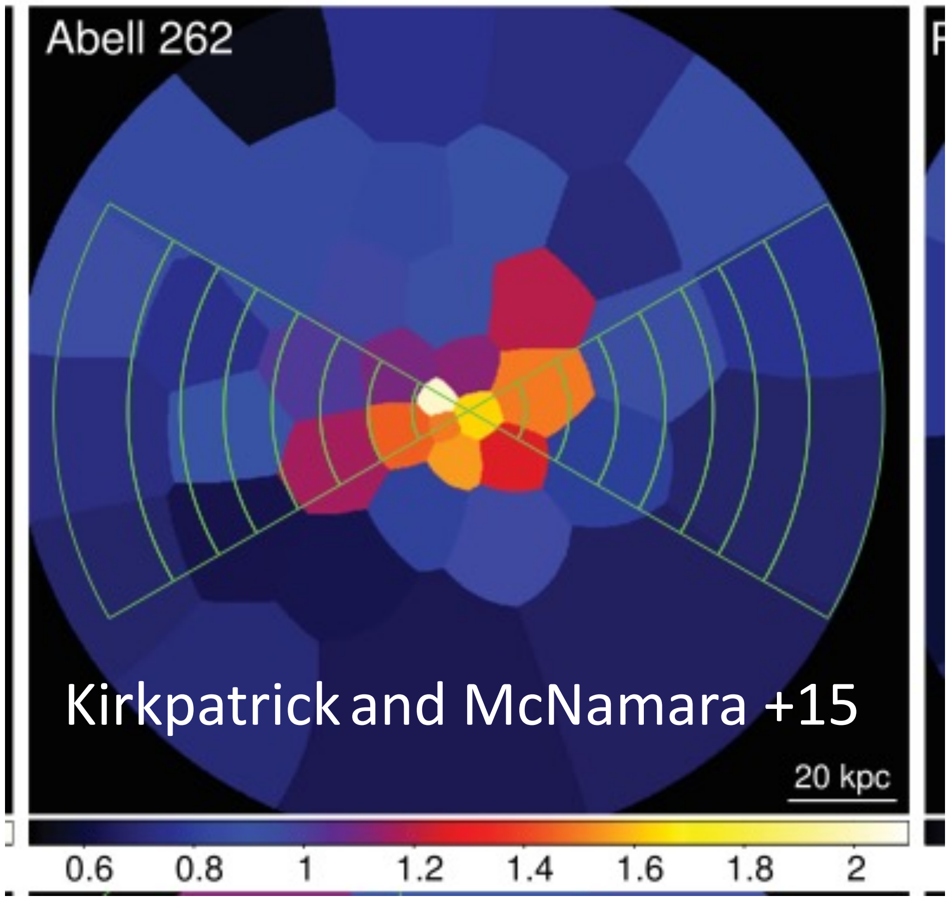

Abell 262
Kirkpatrick and McNamara +15
20 kpc
0.6
0.8
1
1.2
1.4
1.6
1.8
2

Abell 262

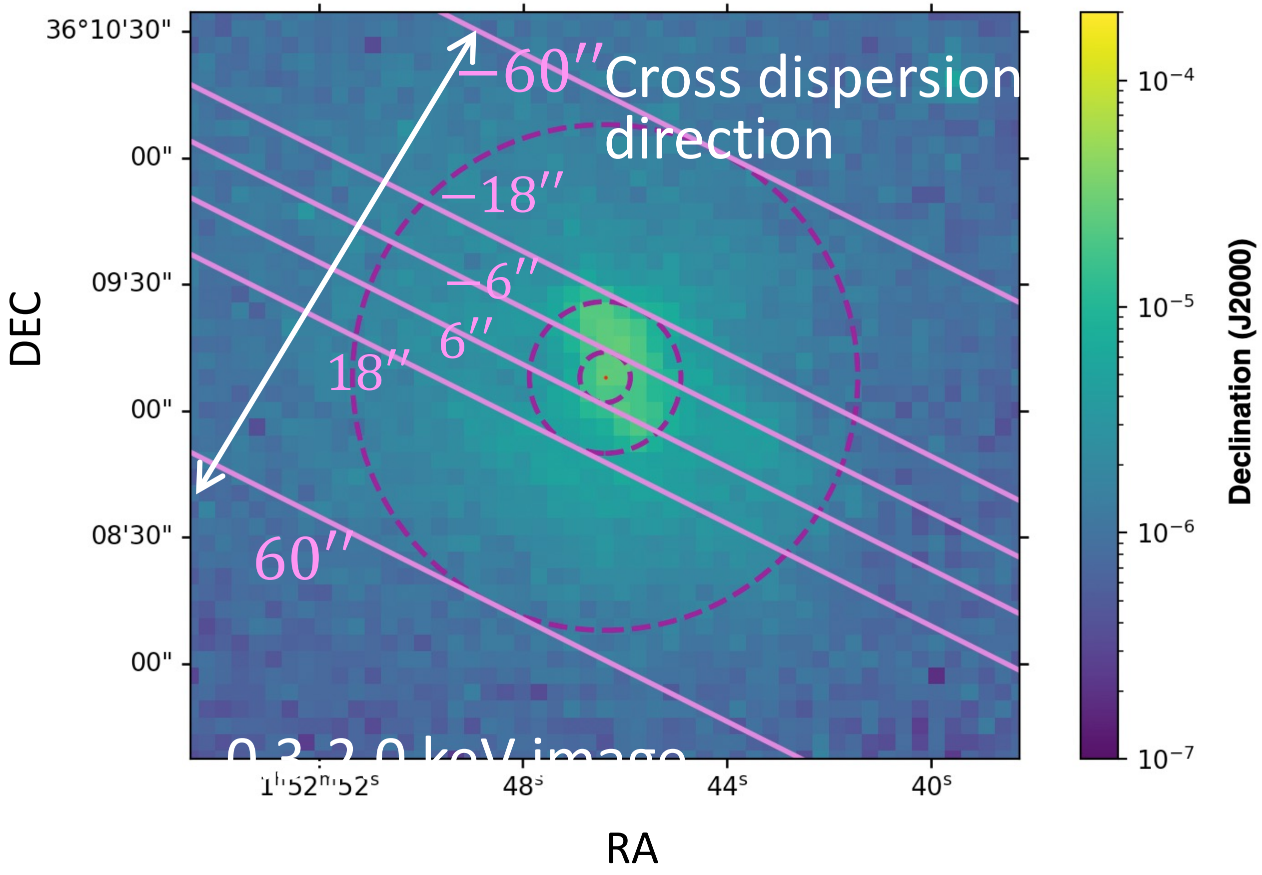

Cross dispersion direction
−60″
−18″
−6″
6″
18″
60″
0.3-2.0 keV image
DEC
RA

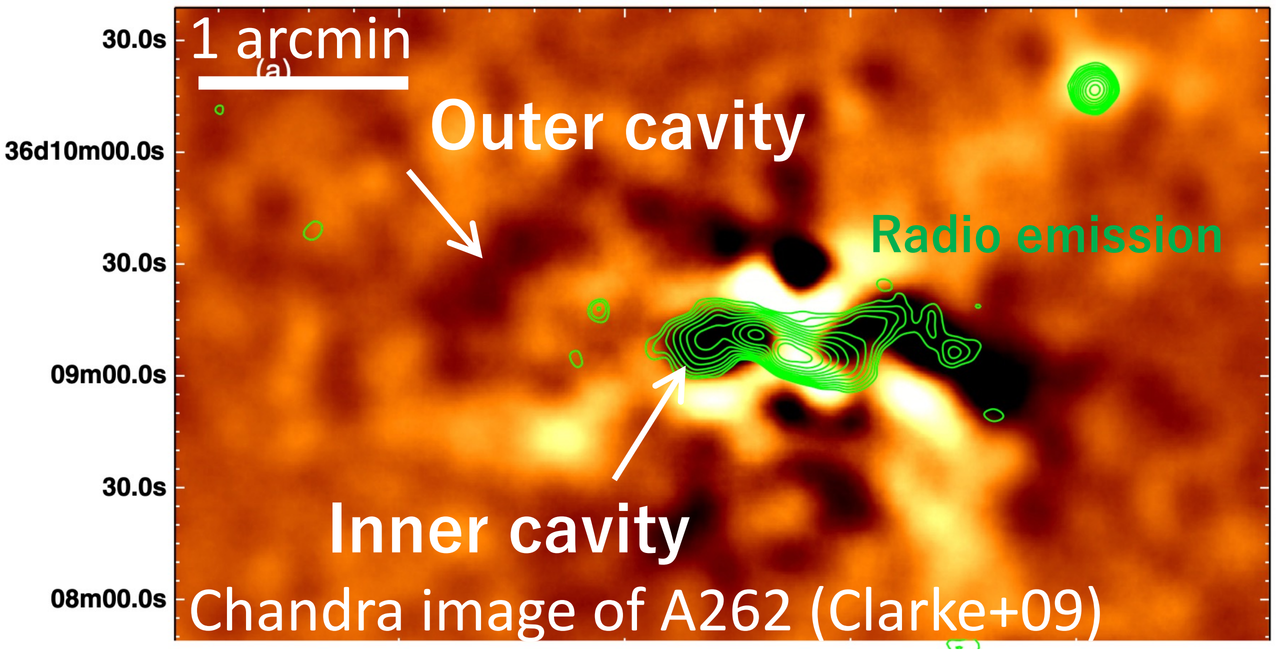

1 arcmin
Outer cavity
Radio emission
Inner cavity
Declination (J2000)
Chandra image of A262 (Clarke+09)

Differences between XSPEC and SPEX

NGC5044

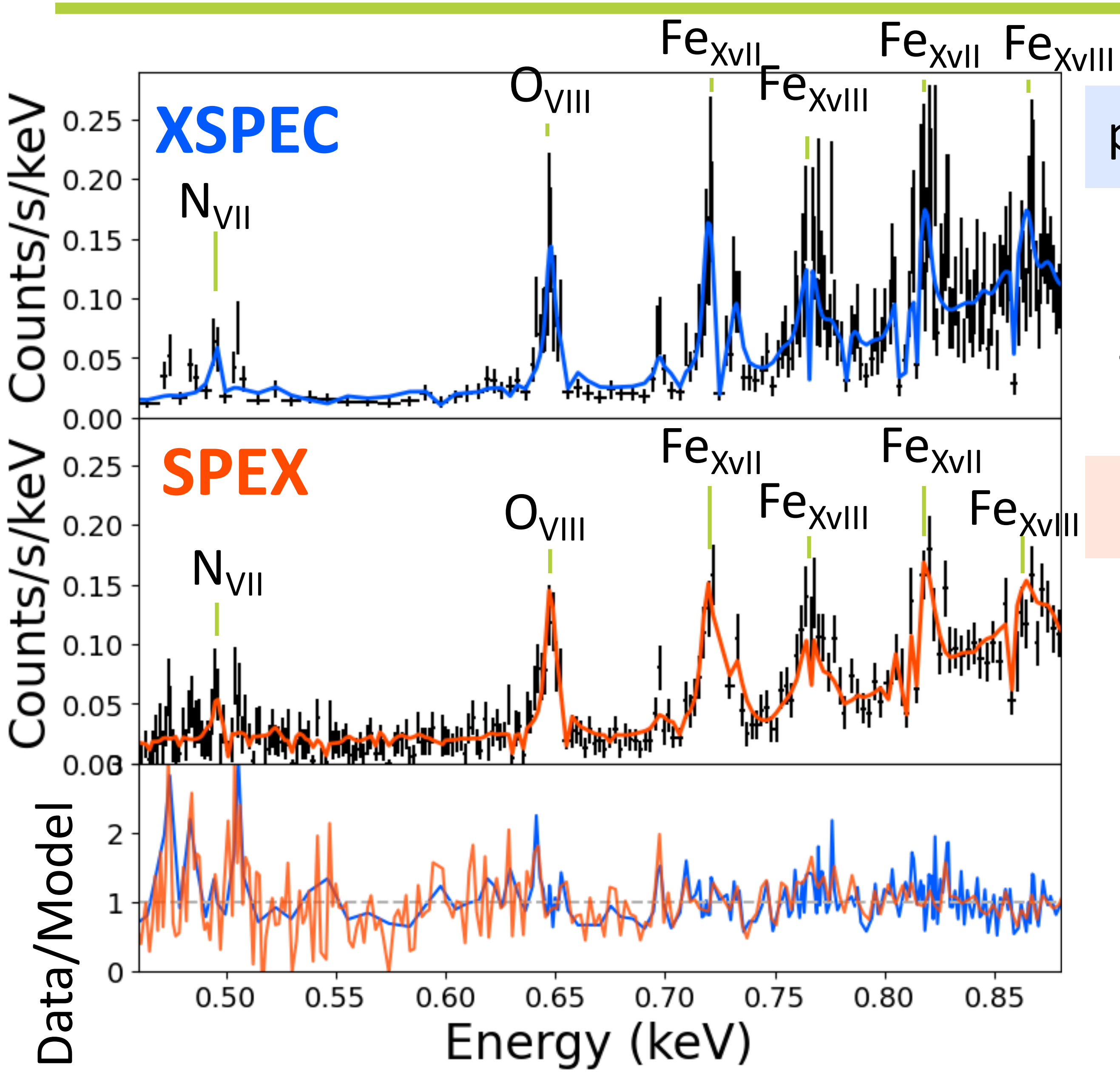

phabs*(**rgsxsrc***bvvapec + **gsmooth***bvvapec)

Line broadening

Binning : 1count/1 bin

Statistic : c-stat

hot***lpro***(cie + cie)

Line broadening

Binning : Optimal binning

Statistic : c-stat

Previous study

Mao et al. 2019

Table 5. Abundance ratios for NGC 5044 within the extraction region (i.e. $\lesssim r/r_{500}$).

X/Fe	Value
N/Fe	1.4 ± 0.3
O/Fe	0.65 ± 0.05
Ne/Fe	0.68 ± 0.08
Mg/Fe	0.77 ± 0.08
Si/Fe†	0.79 ± 0.10
S/Fe†	1.1 ± 0.2
Ar/Fe†	1.0 ± 0.3
Ca/Fe†	1.2 ± 0.2
Fe	0.72 ± 0.02
Ni/Fe	1.5 ± 0.3

Notes. Abundance ratios measured with EPIC spectra are labelled with a dagger.

Previous study

Mao et al. 2019

Table 1. Abundances and abundance ratios within the 3.4 arcmin wide (in the cross-dispersion direction) extraction region.

Source	A 3526	M 49	M 87	NGC 4636	NGC 4649	NGC 5044	NGC 5813	NGC 5846
r/r_{500}	0.026	0.018	0.012	0.022	0.015	0.034	0.031	0.036
kpc	43.2	18.7	17.7	15.6	15.6	37.7	26.9	25.8
Model	NH+2T	GDEM	2T+PL	2T	1T	GDEM	2T	2T
C-stat./d.o.f.	2186/1088	852/544	3954/1111	748/480	1530/1096	1670/1094	2480/1649	1825/1093
$\sigma_{\rm N/Fe}$	$\sim 7\sigma$	$\sim 3\sigma$	$\sim 9\sigma$	$\sim 4\sigma$	$\sim 3\sigma$	$\sim 5\sigma$	$\sim 5\sigma$	$\sim 3\sigma$
N/O	2.7 ± 0.5	2.7 ± 1.0	2.2 ± 0.3	3.3 ± 1.1	2.9 ± 1.0	2.2 ± 0.5	3.2 ± 0.9	2.7 ± 0.8
N/Fe	1.5 ± 0.2	1.6 ± 0.6	1.8 ± 0.2	1.9 ± 0.5	2.4 ± 0.8	1.4 ± 0.3	1.9 ± 0.4	2.3 ± 0.7
O/Fe	0.54 ± 0.04	0.59 ± 0.10	0.82 ± 0.03	0.59 ± 0.08	0.84 ± 0.11	0.65 ± 0.05	0.58 ± 0.07	0.86 ± 0.12
Ne/Fe	0.57 ± 0.06	0.66 ± 0.17	0.55 ± 0.05	0.64 ± 0.12	1.07 ± 0.19	0.68 ± 0.08	0.53 ± 0.09	0.71 ± 0.14
Mg/Fe	0.66 ± 0.07	0.79 ± 0.19	0.24 ± 0.04	0.64 ± 0.13	1.40 ± 0.23	0.77 ± 0.08	0.83 ± 0.11	0.66 ± 0.14
Fe	1.02 ± 0.03	1.50 ± 0.12	0.55 ± 0.01	0.66 ± 0.04	0.55 ± 0.03	0.78 ± 0.03	0.92 ± 0.04	0.77 ± 0.05
Ni/Fe	1.2 ± 0.1	1.8 ± 0.5	0.65 ± 0.07	2.0 ± 0.4	2.5 ± 0.4	1.5 ± 0.3	–	2.0 ± 0.4

Notes. Abundances and abundance ratios are given according to the proto-solar abundance of Lodders et al. (2009). Statistical uncertainties (1σ) are quoted here. Systematic uncertainties on the abundance ratios are estimated in Sect. 4. $\sigma_{\rm N/Fe}$ is the significance level of nitrogen detection according to the N/Fe ratio (to be greater than zero). The uncertainties shown are 1σ statistical error bars. 1T, 2T, and GDEM refer to single-temperature, two-temperature, and multi-temperature DEM distribution (Sect. 3). For A 3526, "NH" refers to a free Galactic hydrogen column density in the spectral analysis. The Galactic hydrogen column densities for the other seven systems are frozen to literature values. For M 87, we use a power law to model the non-thermal component, which varies between the two observations (Werner et al. 2006a). For NGC 5813, the Ni abundance cannot be constrained, and we fix it to solar during the fitting.

Previous study

Mernier et al. 2022 (NGC 1404)

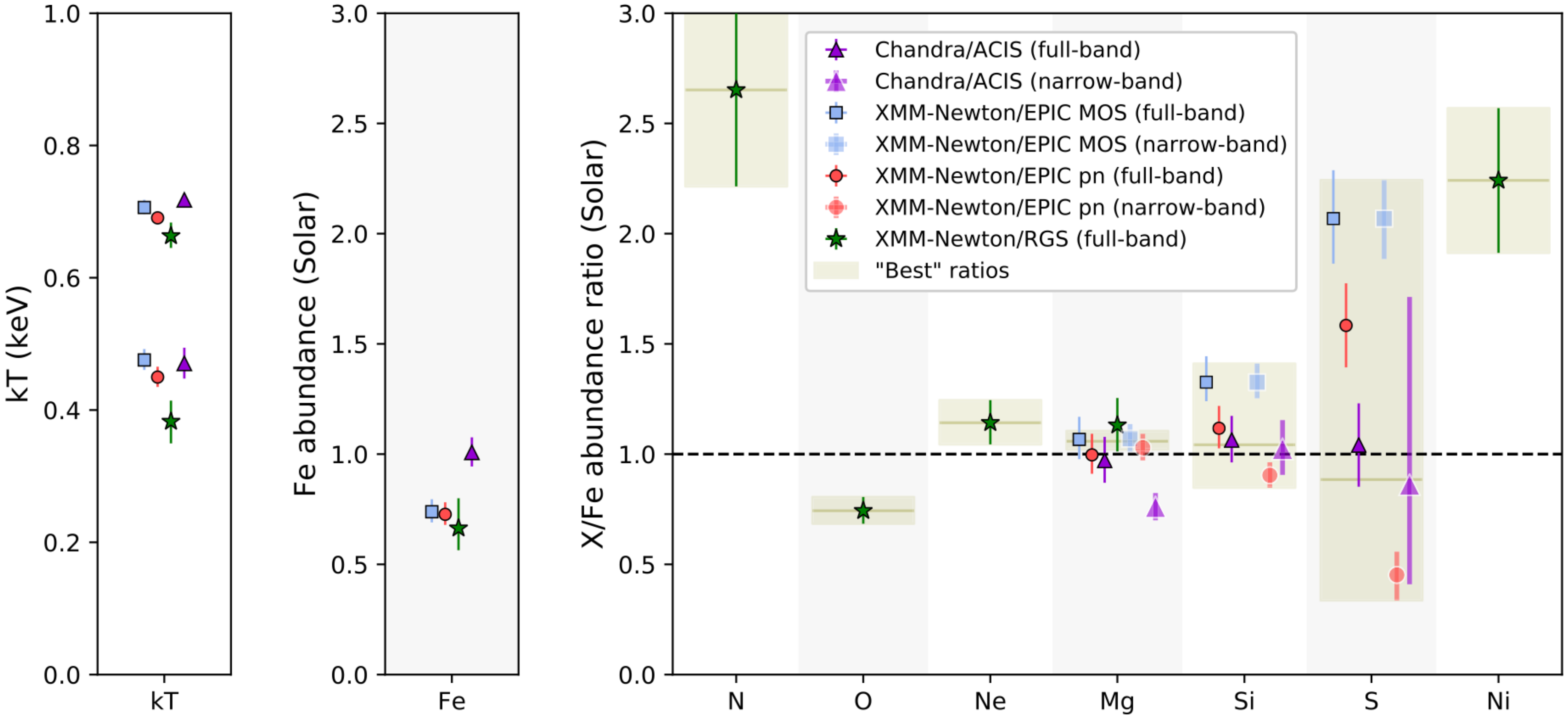

Figure 6. Best-fitting temperatures (kT), Fe abundances, and X/Fe abundance ratios obtained with *XMM–Newton*/EPIC, RGS, and ACIS within a rectangular region covering the RGS extraction region of the deepest *XMM–Newton* observation (see the text and Fig. 3). The MOS, pn, and ACIS measurements are obtained over full-band fits for *kT* and Fe and narrow-band fits for the abundance ratios (see the text).

NGC5044

○ : XSPEC
× : SPEX

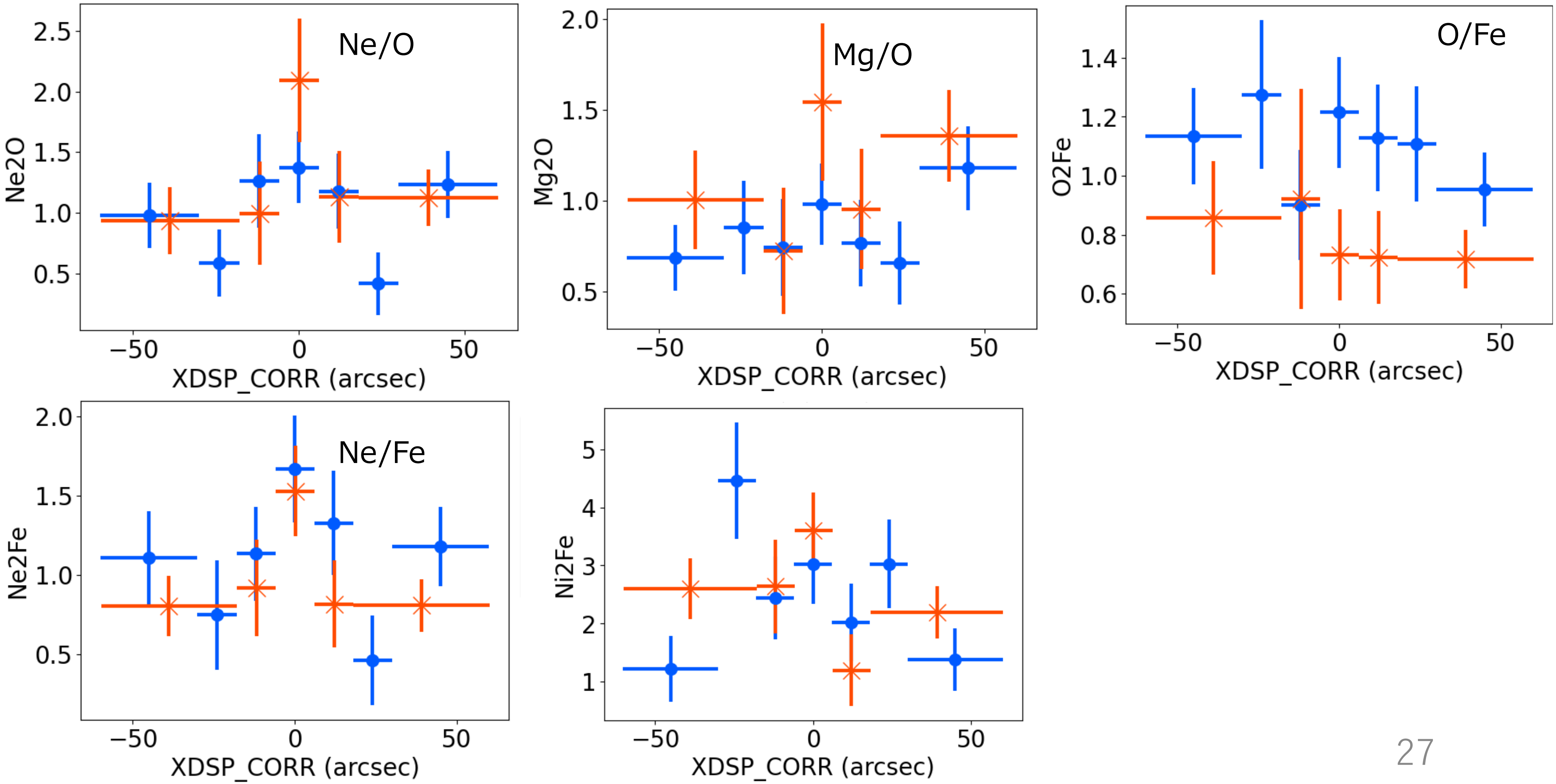

NGC5044

○ : XSPEC
× : SPEX